Contract No:

This document was prepared in conjunction with work accomplished under Contract No. DE-AC09-08SR22470 with the U.S. Department of Energy (DOE) Office of Environmental Management (EM).

Disclaimer:

We put science to work.™

Savannah River National Laboratory™

OPERATED BY SAVANNAH RIVER NUCLEAR SOLUTIONS

A U.S. DEPARTMENT OF ENERGY NATIONAL LABORATORY • SAVANNAH RIVER SITE • AIKEN, SC

Laser Confocal Microscope for Analysis of 3013 Inner Container Closure Weld Region

M. J. Martínez-Rodríguez

October 2017

SRNL-STI-2017-00589, Revision 0

SRNL.DOE.GOV

DISCLAIMER

Printed in the United States of America

Prepared for
U.S. Department of Energy

SRNL-STI-2017-00589
Revision 0

Keywords: *Corrosion*
ICCWR
LCM

Retention: *Permanent*

Laser Confocal Microscope for Analysis of 3013 Inner Container Closure Weld Region

M. J. Martínez-Rodríguez

October 2017

Prepared for the U.S. Department of Energy under contract number DE-AC09-08SR22470.

Savannah River National Laboratory™
OPERATED BY SAVANNAH RIVER NUCLEAR SOLUTIONS

REVIEWS AND APPROVALS

AUTHORS:

M. J. Martínez-Rodríguez, SRNL - Materials Science and Technology Date

TECHNICAL REVIEW:

J. I. Mickalonis, SRNL - Materials Science and Technology Date

APPROVAL:

B. L. García-Díaz, Pu Surveillance Program Lead Date
SRNL - Materials Science and Technology

M. M. Reigel, Manager Date
SRNL - Materials Science and Technology

ACKNOWLEDGEMENTS

The author would like to acknowledge and express gratitude to the following for their assistance in this work: K. E. Hair, G. D. Creech, T. Reown, V. B. Timmerman, and J. G. Duque. Also, the valued guidance from the Materials Identification and Surveillance (MIS) Corrosion Working Group is appreciated.

EXECUTIVE SUMMARY

As part of the protocol to investigate the corrosion in the inner container closure weld region (ICCWR) a laser confocal microscope (LCM) was used to perform close visual examination of the surface and measurements of corrosion features on the surface. However, initial analysis of selected destructively evaluated (DE) containers using the LCM revealed several challenges for acquiring, processing and interpreting the data. These challenges include topography of the ICCWR sample, surface features, and the amount of surface area for collecting data at high magnification conditions. In FY17, the LCM parameters were investigated to identify the appropriate parameter values for data acquisition and identification of regions of interest. Using these parameter values, selected DE containers were analyzed to determine the extent of the ICCWR to be examined.

The parameters considered during the data collection were the image magnification, measurement area (refers to x-y directions in pixels), quality (related to the laser speed), and pitch (refers to the spacing resolution in the z-direction). After evaluation of images and height scan data from different samples with known cracks, the following basic parameters were selected for the examination of the ICCWR with detection of cracks of, at least, 1 μm. Image and height data will be collected on Zone 3 of the ICCWR using 20X magnification, with the double scan function disabled, measurement area set to standard, quality set to high accuracy, and a pitch value of 0.5 μm. Zone 1 and Zone 2 will be examined but images or height data will not be collected unless areas of interest are found. These areas of interest correspond to sections where suspect cracks, significant number of pits or other corrosion features are located. If data collection is necessary for Zone 1 and Zone 2, the double scan function will be enabled. Also, if higher resolution is desired, the parameters can be adjusted accordingly for specific areas of interest.

In order to determine the extent of the ICCWR that requires examination, a metallographic sample of the ICCWR sidewall for FY09 DE09 and a ¼ of the inner container ICCWR sidewall for FY11 HHMC were selected for analysis by LCM. The examination of the ICCWR included analysis up to about 6 mm in Zone 3 from the machining marks towards the bottom of the can, which is the most likely region where cracks can occur. Also, pit depth distributions were analyzed using the Bump Measurement Module (BMM) from the LCM software which can measure concave features in reference to a height specified on the image. The BMM can be used to expedite analysis for evaluation of general condition of the surface but does not distinguish between cracks, scratches or pits. Due to the shallow depth of the baseline container features, the BMM can be used to analyze the deeper corrosion features or pits. However, additional tilt correction may be needed in smaller locations, due to curvature of the sample and the uneven surface. Results from this report show that the corrosion can be extended as far as 6 mm in Zone 3. However, no cracks were detected within the data analyzed.

Also, DE containers from FY13 through FY16 were evaluated to select candidates for a full circumference analysis of the ICCWR. This information will be used to perform a statistical analysis with Los Alamos National Laboratory (LANL) that will help support a determination of how much of an ICCWR needs to be examined and develop an ICCWR sampling plan for analysis of subsequent containers. Based on the results obtained to date the following DE containers were selected for full circumference analysis of the ICCWR with the following prioritization order: FY15 DE07, FY16 DE05, and FY15 DE08. However, this selection can be re-examined and may change in the future as new information becomes available.

TABLE OF CONTENTS

LIST OF TABLES

LIST OF FIGURES

LIST OF ABBREVIATIONS

BMM	Bump Measurement Module
DE	Destructive Examination
FY	Fiscal Year
HAZ	Heat Affected Zone
HHMC	Hanford High Moisture Container
ICCWR	Inner Container Closure Weld Region
LANL	Los Alamos National Laboratory
LCM	Laser Confocal Microscope
MIS	Materials Identification and Surveillance
SCC	Stress Corrosion Cracking
SEM	Scanning Electron Microscope
SRNL	Savannah River National Laboratory
TAM	Testing and Monitoring

1.0 Introduction

The 2014 test plan for assessing the potential of stress corrosion cracking (SCC) of the 3013 inner container was issued by the Materials Identification and Surveillance (MIS) Corrosion Working Group to determine if SCC is plausible within the 50-year design life of a 3013 storage container [1]. One of the main focus areas is a thorough evaluation of the inner container closure weld region (ICCWR) opened for destructive examination (DE), which is part of the 3013 Surveillance Program. A protocol to investigate the corrosion in the ICCWR was developed to characterize the type of corrosion (i.e., mechanisms), the extent of corrosion (percentage of area and depth of attack) and the variables impacting this corrosion (chloride concentration and metallurgical condition) [2, 3]. As part of this protocol a Keyence 3D laser confocal microscope (LCM) model VK-X110 is used to perform close visual examination of the surface at the ICCWR and surface profile measurements for pit depths or other corrosion features on the surface.

Initial analysis of selected DE containers using the LCM revealed several challenges for acquiring, processing and interpreting the data [4, 5]. These challenges can be described in three categories which consist of (a) topography of the ICCWR sample, (b) surface features, and (c) amount of surface area for collecting data at high magnification conditions. The topography of the sample includes curvature of the surface, beveled or steep regions, and uneven surface due to severe corrosion. The surface features are related to differentiating pit-like, crack-like and other baseline features from actual corrosion features. The baseline features correspond to original or pre-corrosion features found on the surface prior to storage conditions. Also, the amount of surface area may require a significant amount of time for collecting and processing the data if the process is not automated.

The above challenges led to several aspects of the corrosion analysis by LCM which needed further examination as listed below:

1. What parameters are required to collect data in order to detect or recognize specific features on the surface?
2. Where, within the sample, does data need to be collected and how much?
3. What techniques are necessary to process the data collected?

Figure 1 shows a diagram relating the different aspects of the corrosion analysis with the sample challenges. In Fiscal Year 2017 (FY17), the LCM parameters were investigated to identify the appropriate parameter values for data acquisition and identification of regions of interest. Using these parameter values, selected DE containers were analyzed to determine the extent of the ICCWR to be examined. Also, DE containers from FY13 through FY16 were evaluated to select candidates for a full circumference analysis of the ICCWR. This information will be used to perform a statistical analysis with Los Alamos National Laboratory (LANL) that will help support a determination of how much of an ICCWR needs to be examined in order to make the assertion of whether or not cracking has occurred and develop an ICCWR sampling plan for analysis of subsequent containers. This report describes the status of the LCM as the technique for the ICCWR examination.

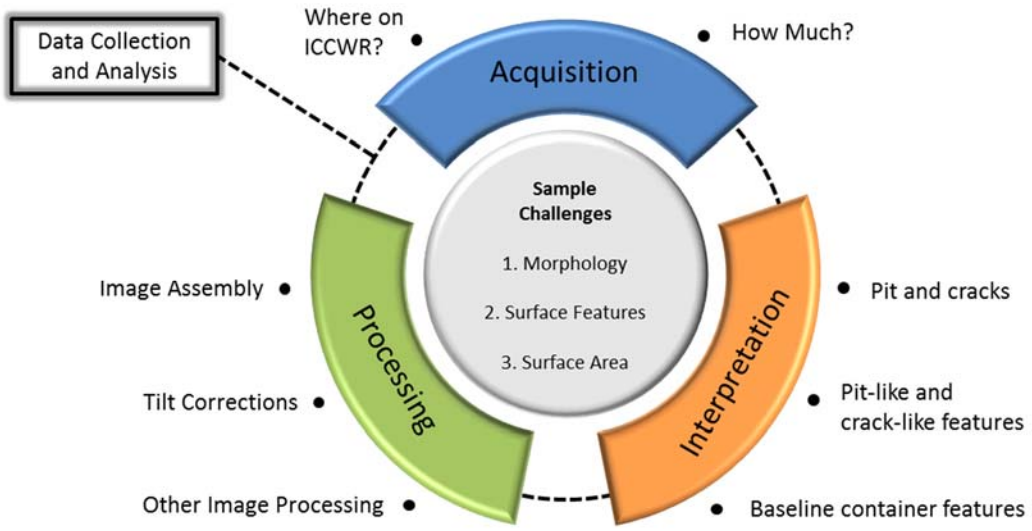

Figure 1. Protocol overview for the examination of the ICCWR.

2.0 LCM Parameters for ICCWR Examination

Previous LCM analysis in the ICCWR show different features on the surface that can be characterized as pits, scratches, dents or suspect cracks, including a baseline container, which showed pit-like and crack-like features on the surface [5]. However, the resolution of the image to detect these features on the surface depends on the LCM parameters selected to collect the data. Consequently, several samples with known cracks of different sizes were imaged to determine the best practical scanning parameters for identifying regions of interest during ICCWR examinations. Throughout this report the 10X, 20X and 50X image magnifications were obtained using the following objective lens, respectively: Nikon 10X/0.30 OFN25 WD 16.5, Nikon 20X/0.35 OFN25 WD 20.5, and Nikon 50X/0.45 OFN25 WD 13.8.

Figure 2 shows the different samples used to image regions with known cracks. These samples consist of a dye penetrant testing and monitoring (TAM) panel with varying sizes of defects, 304 stainless steel sample from crack growth test performed at Savannah River National Laboratory (SRNL) [6], a DE sample from a boiling $MgCl_2$ test performed at SRNL [7], and two teardrops from Cl^--containing gases test performed at LANL [8]. One of the teardrop samples has large cracks while the other has small cracks. LCM images were obtained for cracks located in the TAM panel as shown in Figure 3. However, these spider web-shaped cracks were easily viewed using a 10X magnification. Similarly, the crack in the sample from the crack growth test (Figure 2b) was easily viewed with low magnification images. Therefore, only samples c, d and e in Figure 2 were used to for further analysis.

Images using a 35 mm camera, a stereo microscope and the LCM are shown for the DE sample from a boiling $MgCl_2$ test in Figure 4 and for the teardrops with large and small cracks in Figure 5 and Figure 6, respectively. In each figure, the box with the dash yellow line on the 35 mm picture denotes the area covered by the stereo microscope image and the smaller box with the solid red line denotes the LCM image, which is the highest magnification of the set of images. The 35mm picture and the stereo microscope image in Figure 4 show multiple regions of interest but the size and depth of the features cannot be determined. For the teardrops, all the images show cracks on

the samples, but the 35 mm pictures and the stereo microscope image show only the wider cracks (> 10 μm), most noticeable in the stereo microscope image. Mid-width cracks, in the range of 3 – 5 μm, can be observed if the LCM is used at a 10X magnification (white circle in Figure 5c). Narrower cracks of about 1 μm can be observed when the LCM is used at a 20X magnification. Cracks narrower than 1 μm can be observed if the LCM magnification is increased to 50X, as shown in Figure 6c, but cannot be measured due to software limitation. Crack widths are measured from the image with the LCM software but if the width is less than the minimum digital spacing of 1 μm then it cannot be measured. The crack widths that can be observed are summarized in Figure 7, which shows LCM images at three magnifications, 10X, 20X and 50X, for the teardrop with smaller cracks. At 10X crack widths > 3 μm can be seen and measured. At 20X cracks > 1 μm in width can be seen and measured. At 50X cracks < 1 μm can be observed but not measured.

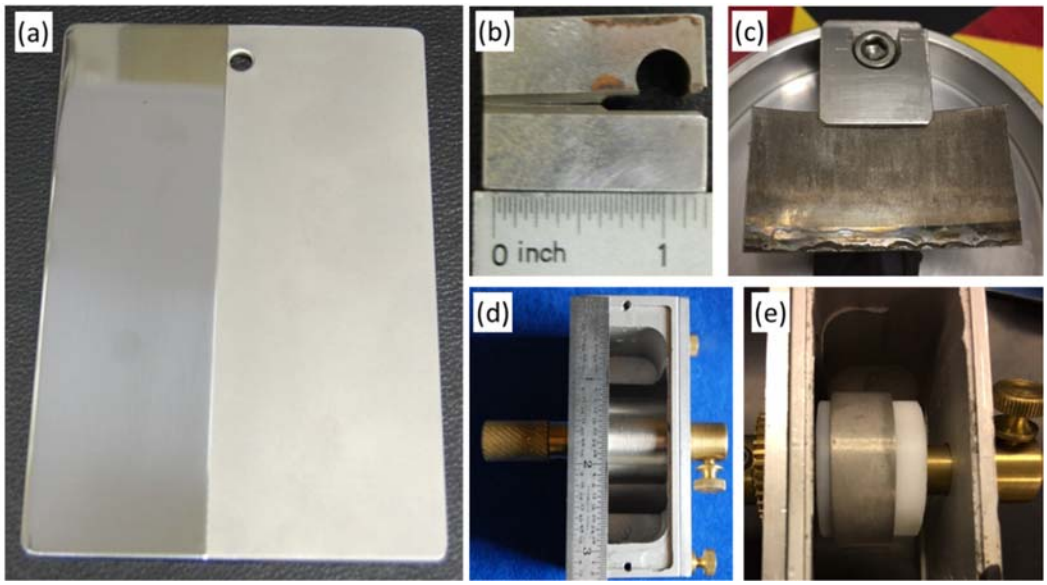

Figure 2. Samples used for crack measurements: (a) TAM panel with varying sizes of defects, (b) 304 stainless steel sample from crack growth test (SRNL), (c) DE sample from $MgCl_2$ test (SRNL), teardrops from Cl-containing gases test (LANL) with (d) large cracks and (e) small cracks.

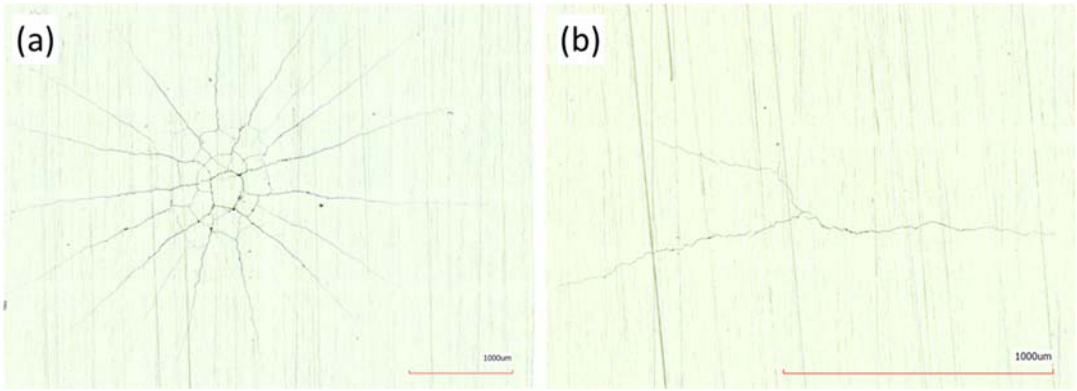

Figure 3. LCM images showing cracks from two defects in the TAM panel (a) at 10X magnification and (b) 20X magnification.

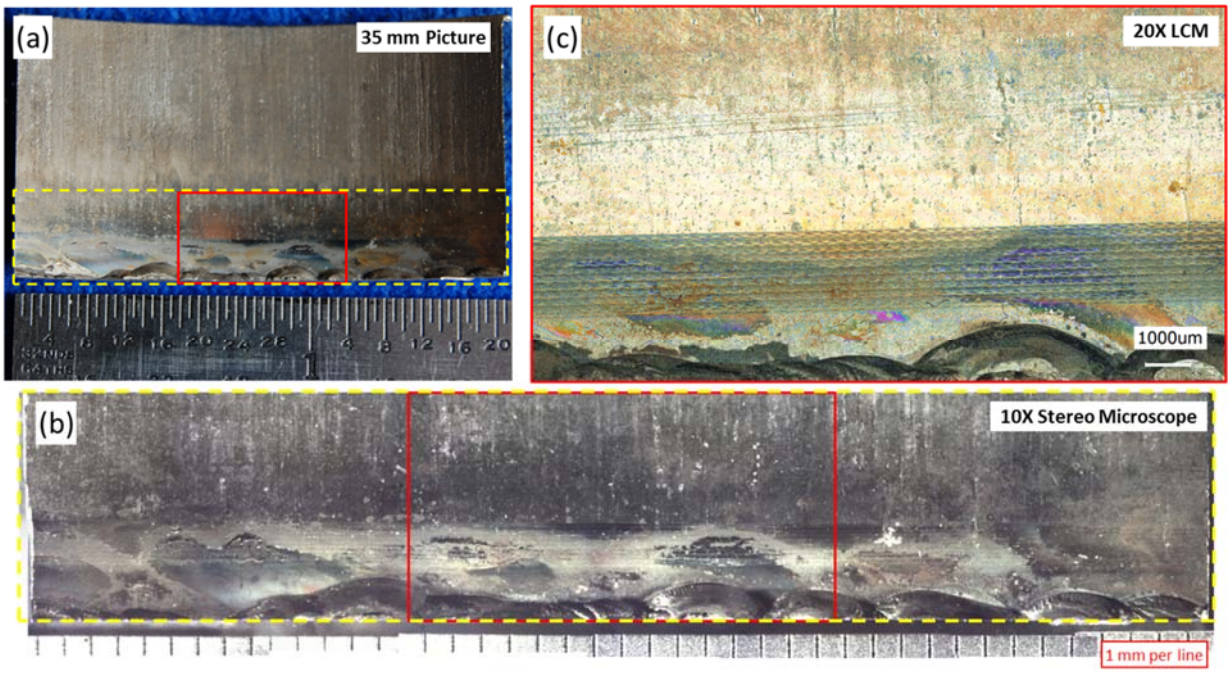

Figure 4. Images of DE sample from $MgCl_2$ test using (a) 35 mm camera, (b) stereo microscope at 10X and (c) LCM at 20X.

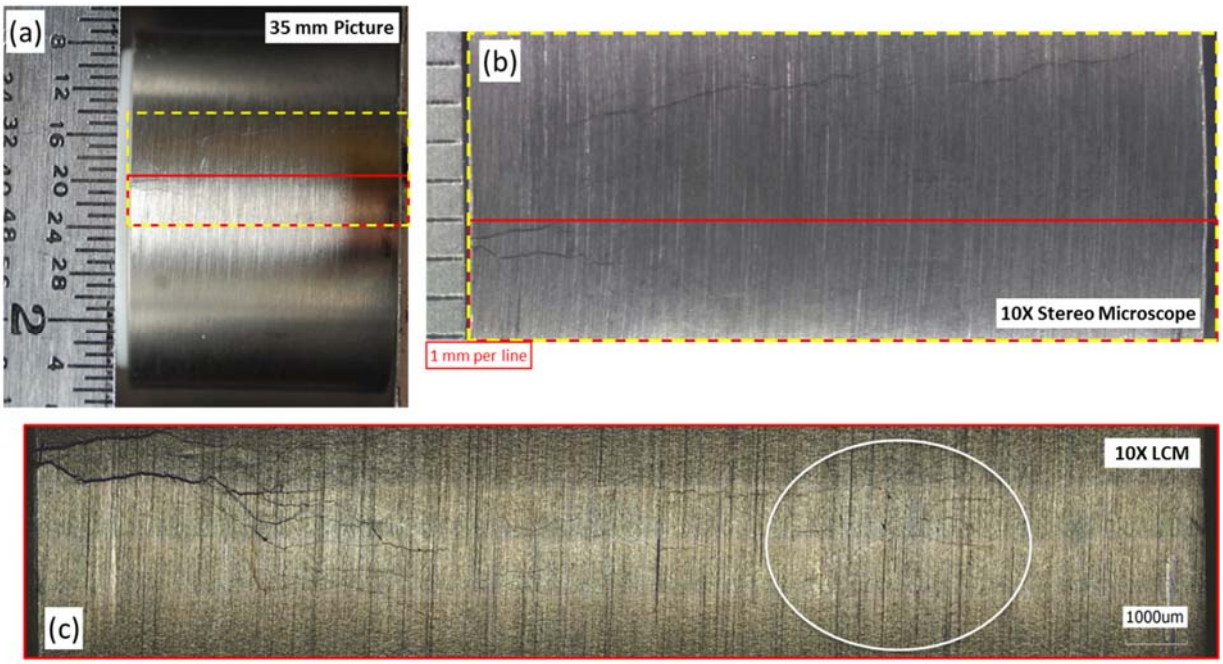

Figure 5. Images of teardrop with large cracks from Cl-containing gases test using (a) 35 mm camera, (b) stereo microscope at 10X and (c) LCM at 10X.

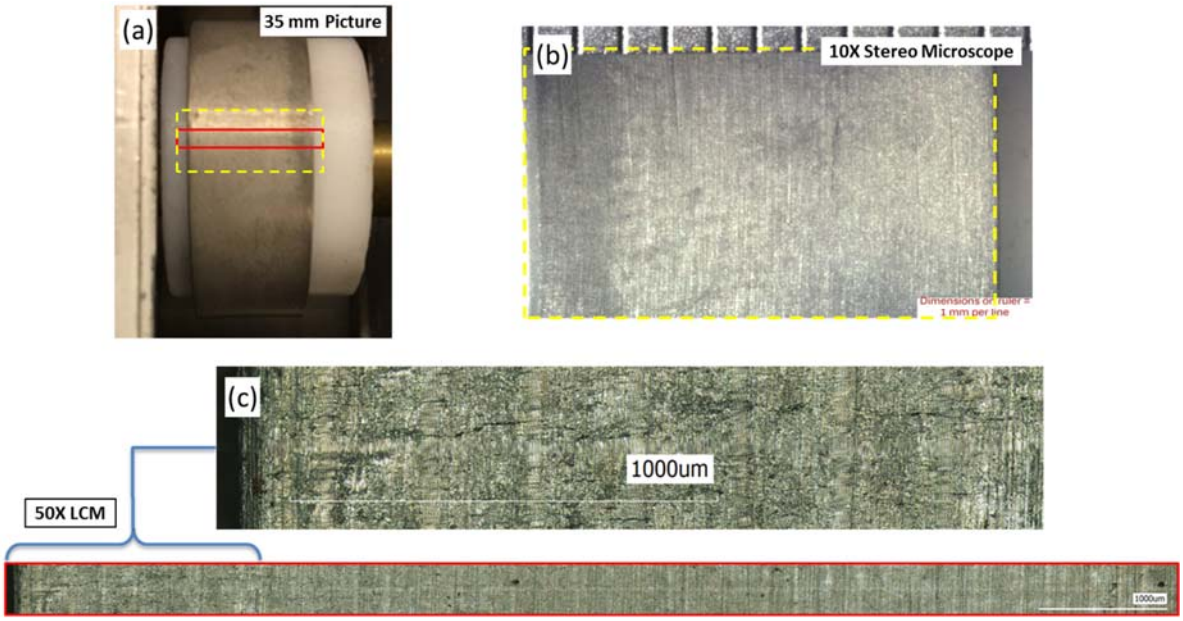

Figure 6. Images of teardrop with small cracks from Cl-containing gases test using (a) 35 mm camera, (b) stereo microscope at 10X and (c) LCM at 50X.

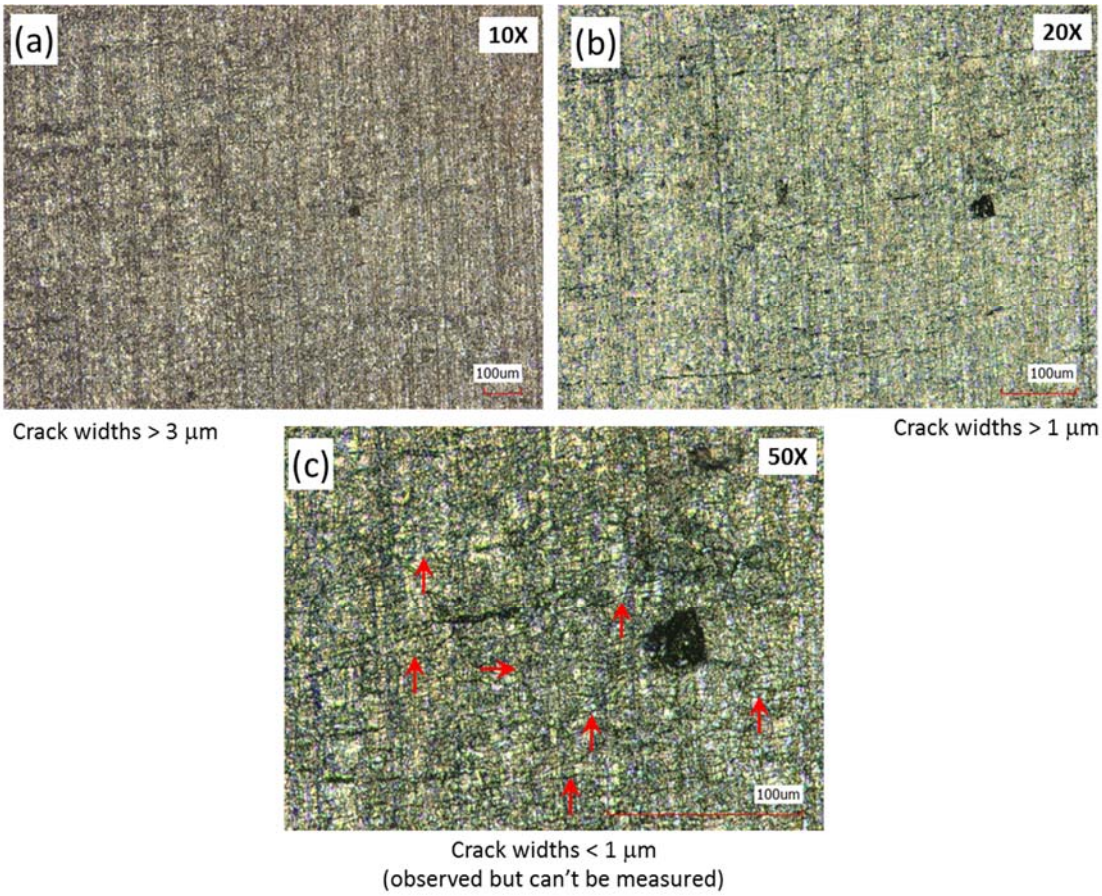

Figure 7. Images of teardrop with small cracks from Cl-containing gases test using an LCM at (a) 10X, (b) 20X and (c) 50X.

Another aspect for selecting the best practical parameters for the LCM is the topography of the DE sample at the ICCWR. Figure 8 shows a representative Scanning Electron Microscope (SEM cross-section image of the ICCWR. Once the weld is removed to separate the lid section from the sidewall section, the surface of the sidewall, as indicated by the red box in Figure 8, will have a general profile as shown in Figure 9a. In the weld fusion zone, the weld beads on the surface resemble valleys and mountains (see Figure 4). In the heat affected zone (HAZ) the surface is mostly flat with a beveled region where the machining marks are located. These regions are divided in three zones as shown in Figure 9b. The fusion zone is considered Zone 1, the region with machining marks is considered Zone 2 and the flat portion of the HAZ is considered Zone 3.

The LCM has a double scan function for samples with steep angles, such as Zone 1 and Zone 2. This function enables measuring under normal brightness conditions during the first scan and with an increased brightness during the second scan [9]. This allows the software to collect data within the steep angle regions with minimal noise. However, the use of the double scan function will also double the amount of time to collect data. For Zone 3 the use of the double scan is not necessary because this zone is mostly flat. In order to save time during data collection, it is possible to examine Zone 1 and Zone 2 using the LCM without collecting data while data can be collected for Zone 3 without using the double scan function. If features of interest are noted in Zone 1 and Zone 2 then it is possible to collect data on those specific areas using the double scan function.

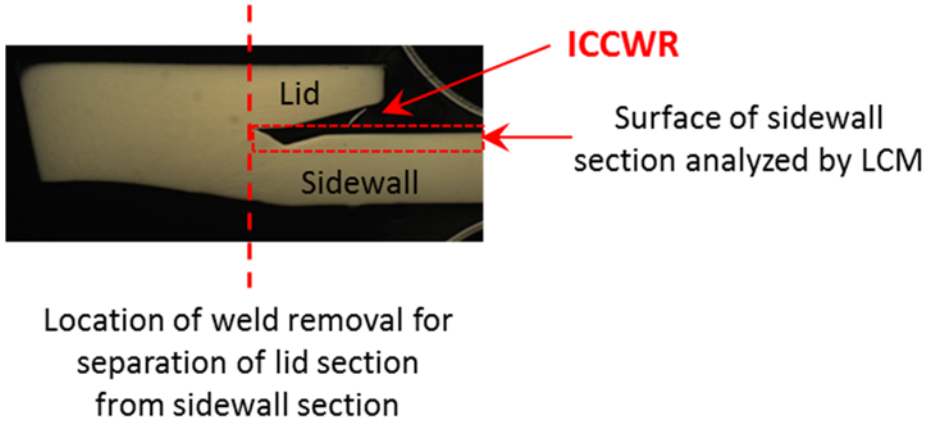

Figure 8. Representative SEM cross-section image of the ICCWR.

Even for Zone 3, the characteristics of the surface of DE samples can affect the LCM scanning parameters, data collection time and data processing. Figure 10 shows the optical images and the height scans for the ICCWR sidewall Zone 3 obtained from four DE samples: baseline container, FY14 DE02-B2[1], FY11 HHMC-90°[2], and the DE sample from the boiling $MgCl_2$ test. From left to right the order of these samples shows the progression of corrosion and the changing in surface features encountered. The baseline container shows features on the surface that can be characterized as pit-like and crack-like features. These features are intrinsic to the container and

[1] The inner container lid is cut in 4 sections labeled A, B, C and D starting from the weld overlap and following a clockwise direction when the lid is oriented facing the interior surface. The quarter section B was cut further into 1/8 sections of the can lid, labeled B1 and B2, to fit the LCM box for examining contaminated samples.
[2] When metallographic samples are cut from the inner container lid, they are labeled with the approximate degree from the position cut. The weld overlap corresponds to 0° and the increases in the clockwise direction when the lid is oriented facing the interior surface. The Hanford High Moisture Container (HHMC) is known for the high moisture condition during storage.

are not related to corrosion. FY14 DE02-B2 is a container that has been exposed to the 3013 storage conditions and still shows similar pit-like features as the baseline container. Both, the baseline and FY14 DE02-B2, show features with depths of 4 ± 2 μm. The FY11 HHMC-90° shows surface corrosion observed at the bottom of the optical image (Figure 10e) where the HAZ tint on the surface has been partially lost. Also, the height scan (Figure 10f) shows varying colors indicating the surface is rougher from corrosion damage. Surface features can be observed on the image but some of the features are deeper than the baseline features indicating actual pits or corrosion. For this sample, the average surface feature depth is 15 ± 4 μm. The boiling $MgCl_2$ test sample shows more corrosion than FY11 HHMC-90° and includes a crack that can be observed in the optical image and height scan. The average surface features depths are 18 ± 5 μm.

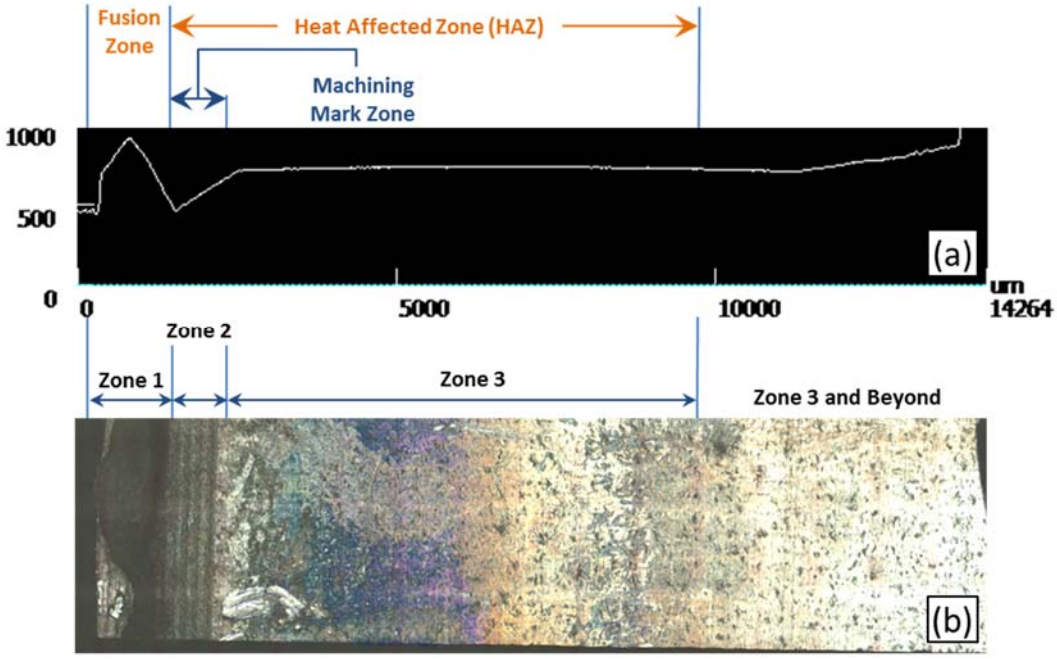

Figure 9. General topography of an ICCWR sidewall sample. Image of FY11 HHMC-90° sidewall showing (a) side view of surface profile and (b) top view optical image of surface [5].

Additional parameters considered during the data collection were the measurement area (or size), quality, and pitch. The measurement area refers to the 2D plane (x-y directions) and can be set to standard (1024 x 768 pixels) or super fine (2048 x 1536 pixels). The quality is related to the laser speed, which includes high accuracy (9 Hz), high speed (15 Hz), and ultra-high speed (25 hz). Under high accuracy the laser scans every line left to right of the measurement area, in high speed the laser scans left to right but skips every other line, and in ultra-high speed the laser scans left to right, skips a line, scans right to left, skips a line, and so on. In high speed and ultra-high speed the unmeasured lines are interpolated from the adjacent lines [9]. The pitch refers to the spacing resolution in the z-direction.

Table 1 shows the estimated scanning time to cover approximately 0.37 mm^2 of the ICCWR Zone 3 at 20X magnification when different set of parameters are used. The quality was set to high accuracy and kept constant in order to raster across the entire surface and avoid the interpolation

between scanned lines. Selecting double scan vs single, super fine vs standard or doubling the pitch value will also doubles the scanning time for each parameter change. Consequently, the parameter values for the measurement area, quality and pitch were selected as to maintain a balance between image resolution and acquisition time. As described above, the double scan can be used when it is necessary. At 20X magnification, a standard pixel area produces a resolution of about 0.7 μm/pixel. For the pitch, a value of 0.5 μm is sufficient to measure a feature depth within micron resolution.

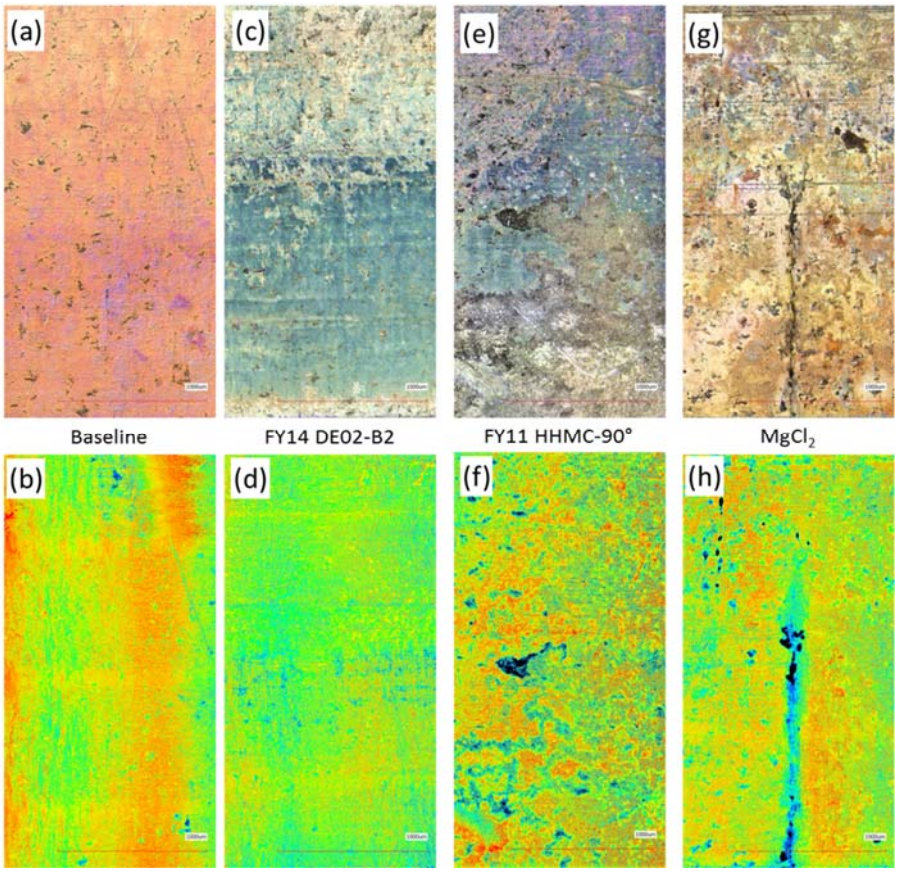

Figure 10. Optical images (top) and height scans (bottom) of ICCWR sidewall Zone 3 from DE samples. Increasing height is represented by transition in color from blue (lowest) to red (highest). DE samples correspond to (a)/(b) baseline container, (c)/(d) FY14 DE02-B2, (e)/(f) FY11 HHMC-90°C and (g)/(h) DE from boiling $MgCl_2$ test.

Based on the information presented above the following basic parameters were selected for the examination of the ICCWR with detection of cracks of, at least, 1 μm. Image and height data will be collected on Zone 3 of the ICCWR using 20X magnification, with the double scan function disabled, measurement area set to standard, quality set to high accuracy, and a pitch value of 0.5 μm. Zone 1 and Zone 2 will be examined but images or height data will not be collected unless areas of interest are found. These areas of interest correspond to sections where suspect cracks, significant number of pits or other corrosion features are located. If data collection is necessary for Zone 1 and Zone 2, the double scan function will be enabled. Also, if higher resolution is desired, the parameters can be adjusted accordingly for specific areas of interest.

Table 1. Estimated time of scan to cover 0.37 mm^2 on ICCWR Zone 3 at 20X for differet sets of LCM parameters.

Double Scan	Yes	No	Yes	No
Area (Size)	Super Fine	Super Fine	Standard	Standard
Quality	High Accuracy	High Accuracy	High Accuracy	High Accuracy
Pitch (µm)	Measurement Time (min)			
0.2	8	4	4	2
0.5	4	2	2	1
1	2	1	1	0.5
2	1.5	0.75	0.75	0.375

3.0 Extent of ICCWR Examination

The examination of the ICCWR will include the most likely regions where cracks can occur. During the boiling $MgCl_2$ tests conducted at SRNL, SCC was observed on SRS/Hanford inner containers [7, 10]. The exterior of the ICCWR showed vertical cracks extended from the weld to approximately 5 – 9 mm below the weld. These cracks were consistent with residual hoop stresses measurements performed at LANL which indicated that the highest observed hoop stresses were located at 2.5 mm below the weld as measured with the incremental hole drilling method and at 4 – 5.5 mm below the weld as measured with the contour method [11]. The location of these cracks, within the interior of the ICCWR, is shown in the LCM optical image in Figure 11. The weld (not shown in Figure 11) is located below Zone 2 as can be observed in Figure 4c. Figure 11 indicates that most of the cracks are in Zone 3 with only a small part extending to Zone 2. Zone 3 starts about 3 – 4 mm from the weld (see Figure 4c), which put the observed cracks within the range of the maximum residual stresses. Since cracks can extend 9 mm below the weld and Zone 3 can starts at 3 mm below the weld, initial analysis of ICCWR will extent to 6 mm in Zone 3.

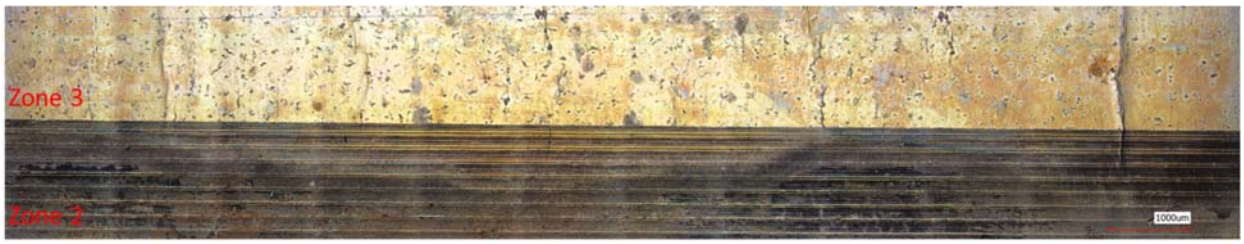

Figure 11. Optical image of ICCWR sidewall Zones 2 and 3 of DE container from boiling $MgCl_2$ test. Note that the picture is oriented such that the weld is below Zone 2.

To explore more details for determining the extent of the ICCWR that requires examination, a metallographic sample of the ICCWR sidewall for FY09 DE09 and a ¼ of the inner container ICCWR sidewall for FY11 HHMC were selected for analysis by LCM. These samples were cleaned by using 2.0 M HNO_3 solution and sonication for 60 min at 60°C. The samples were placed in a DE sample holder (LCM box) as described by Martínez [5]

In addition, an LCM analysis was performed for the DE baseline to differentiate the actual corrosion features on the surface of DE samples from the DE baseline features. Figure 12 shows examples of the LCM optical image and height scan for the surface of the DE baseline. These

images show pit-like features or dark spots or regions on the surface. The depth of these features was measured using the LCM software on 30 images that were selected randomly. The results are presented in Figure 12c as pit-like depth distribution based on the maximum pit-like depth found on each image and for all pit-like features. For either case, the measured depths are less than 8 μm. Consequently, baseline features can be disregarded by performing the analysis on corrosion features of interest deeper than 8 μm

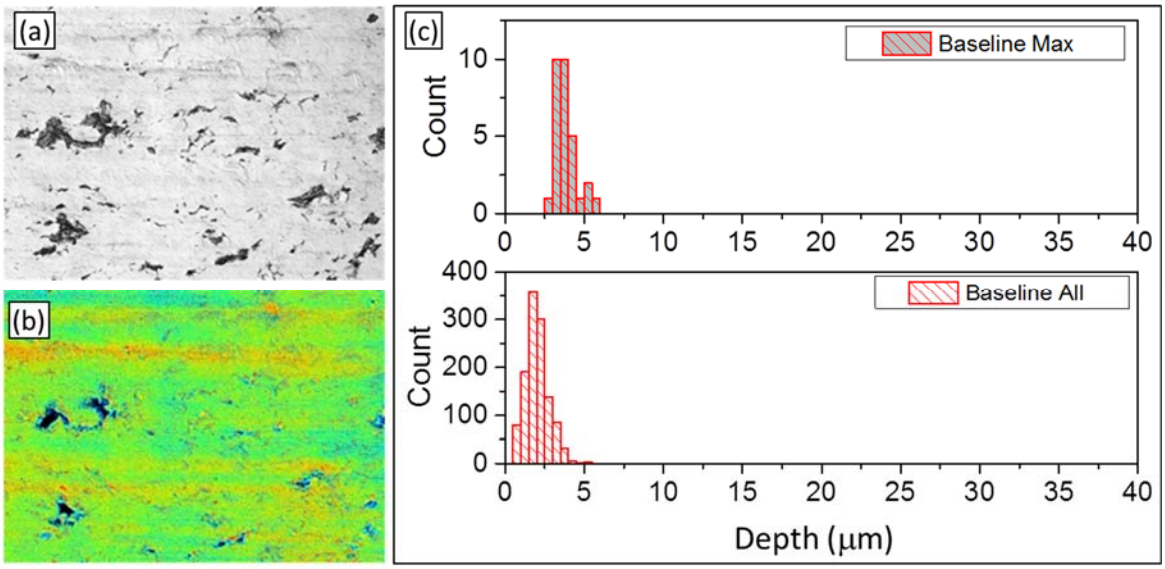

Figure 12. LCM analysis of 30 images from the DE baseline [12] showing (a) optical image example, (b) height scan example, and (c) pit-like depth distribution for maximum pit-like depth (Max) on each individual image and for all pit depths (All). Increasing height is represented by transition in color from blue (lowest) to red (highest).

3.1 ICCWR Examination of FY09 DE02

FY09 DE02 is the inner container known for the halo of pits in the interior surface of the lid [13]. Analysis by stereo microscope and SEM have shown general corrosion and pitting within the ICCWR [2] which make these samples ideal for analyzing the extent of the ICCWR sidewall that needs examination by LCM. The metallography sample FY09 DE02-270° sidewall was selected for analysis by LCM. This sample, although labeled or intended to be cut at 270°, actually corresponds to the section between 285° and 297°, as shown in Figure 13.

Initial analysis for FY09 DE02-270° sidewall was performed up to about 6 mm in Zone 3 from the machining marks towards the bottom of the can (i.e. sample is oriented with the weld facing down). The intent is to evaluate if 6 mm is sufficient to cover the most likely area to find cracks, as discussed above, or if the vertical extent can be reduced to 4 mm. Decreasing the extent of examination to 4 mm can greatly reduce the amount of time and storage space to collect and process data. However, if enough corrosion evidence is found beyond 4 mm then the extent of examination will remain at 6 mm. Figure 14 shows an optical image of the section analyzed by LCM for FY09 DE02-270° sidewall. The sample is about 12 mm wide. It shows a rough surface in Zone 3 and partial loss of the HAZ tint due to corrosion. Baseline features, as shown in Figure 12a, can be observed on the sample in Figure 14. In addition, scratches and crack-like features can

be observed in Zone 3 just above the machining marks. A region enclosed by a red box in Figure 14 is magnified in Figure 15 presenting a closer view of the suspect cracks (labeled as A and B) along with other vertical marks or scratches. Further analysis of the region just above the machining marks, such as SEM or cross-sections by serial metallography, is required to investigate if these features are cracks.

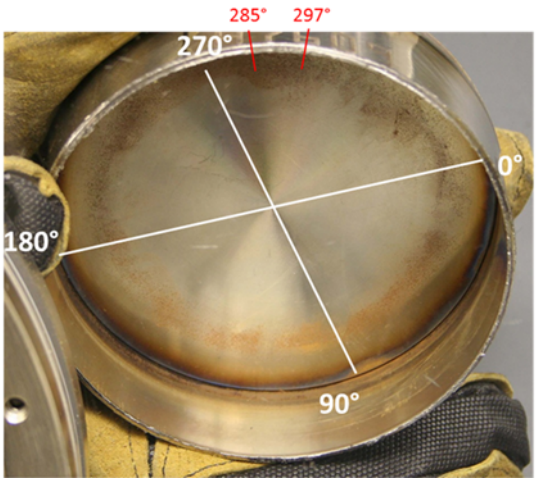

Figure 13. Inner container top lid of FY09 DE02 showing the section corresponding to the ICCWR sample cut for metallography analysis. This sample was labeled as 270° but it actually corresponds to the section between 285° – 297°. The weld overlap corresponds to 0°.

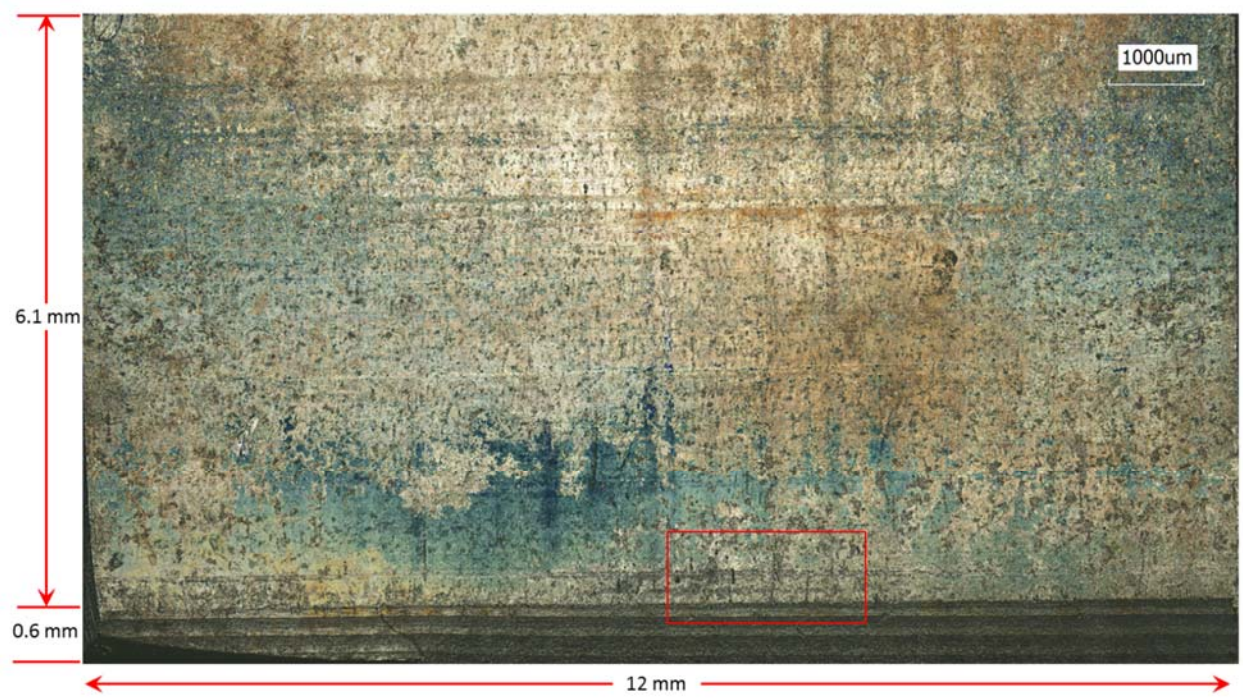

Figure 14. Optical image of FY09 DE02-270° ICCWR sidewall showing Zone 2 (machining marks region measuring 0.6 mm) and Zone 3 (region measuring 6.1 mm above machining marks). Note that the picture is oriented such that the weld (not shown) is below Zone 2. Red box corresponds to image section shown in Figure 15.

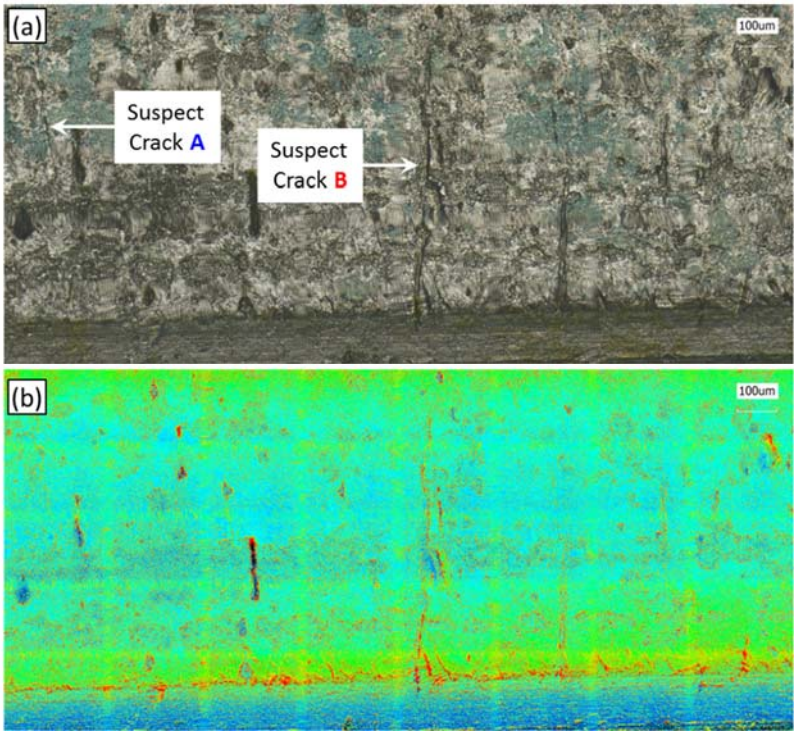

Figure 15. Magnification to 50X of region enclosed by the red box in Figure 14 for FY09 DE02-270° showing (a) optical image and (b) height scan.

The optical image shown in Figure 14 is an assembly of several images of standard resolution (1024 x 768 pixels). The sections corresponding to Zone 3 and the top of Zone 2 of this assembly are shown in Figure 16 as a montage composed of 300 images (15 rows x 20 columns). The approximate angle position, as related to Figure 13, is noted below the image in Figure 16 for reference purposes. Due to software limitations on the maximum number of images that can be assembled without losing resolution, the overall image has to be reassembled in smaller regions labeled 1 through 12 as shown in Figure 16. The maximum number of individual images that can be assembled cannot exceed 25,160,256 pixels in the final assembled image. Otherwise, the software will adjust the size to be less than that by skipping data automatically (collecting the data from every few lines) [14]. As described in Appendix A, the maximum image assembly (vertical x horizontal) size that can be stitched is about 6 x 6 images at 20X (1024 x 768 pixels) to retain the original resolution of the individual images. Figure 16 shows that regions 1 through 12 were selected as assemblies of 5 x 5 images.

Reassembled regions, as noted in Figure 16, were used to analyze the pit depth distribution. These regions were analyzed using the Bump Measurement Module (BMM) from the LCM software. This module measures an area that is higher (convex) or lower (concave) than the height specified in the software for the image [15]. For purpose of measuring the pit depths, the module was set to concave measurements and the height threshold was defined as 8 μm below the average surface level. That is, the module measured concavities with depths of more than 8 μm. The 8 μm was selected as to avoid measurements of the baseline features noted in Figure 12. The average surface level was selected as the mode value of the height data range of the surface. Figure 17 shows an example representing a surface with height data range between 17 and 126 μm and a mode value

of 60 μm. For this example, the height threshold for the BMM will corresponds to 52 μm. Consequently, any depth values from the BMM, obtained using a height threshold of 8 μm below the average surface level, was corrected to the true depth by adding back 8 μm. In addition, due to uneven surface or concavity of the overall DE sample, even after tilt corrections to the surface during the image pre-processing, areas within the image can still show sections that are too low with respect to the overall average surface level. These sections make difficult to separate shallow features within that local region, such as the baseline features, from deeper corrosion features of interest. This requires dividing the image into smaller sections, as shown in Figure 18, where each section is tilt corrected and processed with its local average surface level.

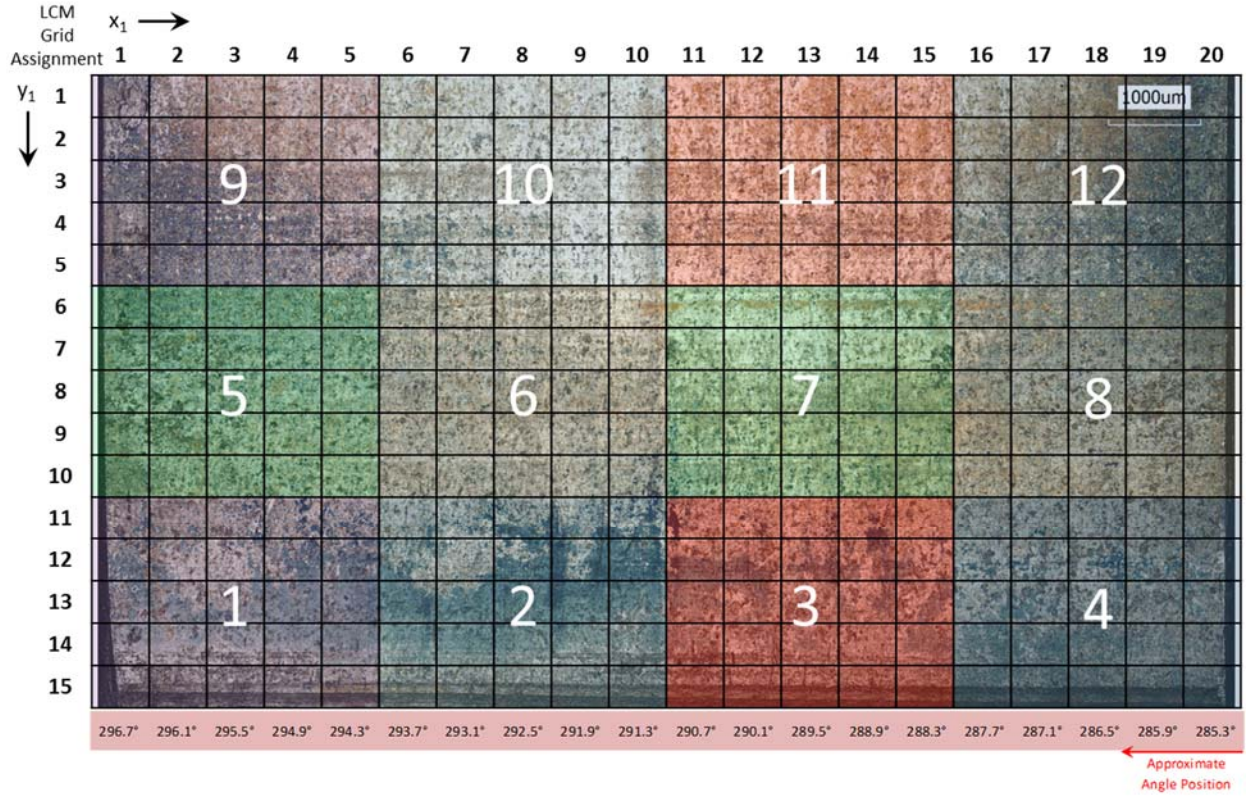

Figure 16. LCM image assembly composed of 300 individual images for FY09 DE02-270° ICCWR sidewall sample showing reassembled regions (1 – 12) for further analysis.

Pit depth distributions for each of the 12 regions displayed in Figure 16 are shown in Figure 19. Pit depths, as measured with the BMM, are generally less than 25 μm. Also, the number of pits is larger in the sections of Zone 3 closer to Zone 2 (regions 1 to 4) and decreases as the section in Zone 3 is farther away from Zone 2. Overall pit depth distribution is shown in Figure 20. The deepest pit found was 33 μm and the largest count was 14 corresponding to pits with depth of 13 μm.

Although this analysis provides an initial estimate of the pit depth distribution, further analysis is being performed with individual images, rather than an assembly of images. Due to the curvature of the sample and the uneven surface, the assembled image needs to be divided into smaller sections to apply tilt corrections. Smaller sections than those shown in Figure 18 may be more precise and adequate to minimize uncertainty on the measurements. Yet this also increases the

amount of data processing due to the number of individual images analyzed. Consequently, alternative techniques are being investigated to process the data from individual images.

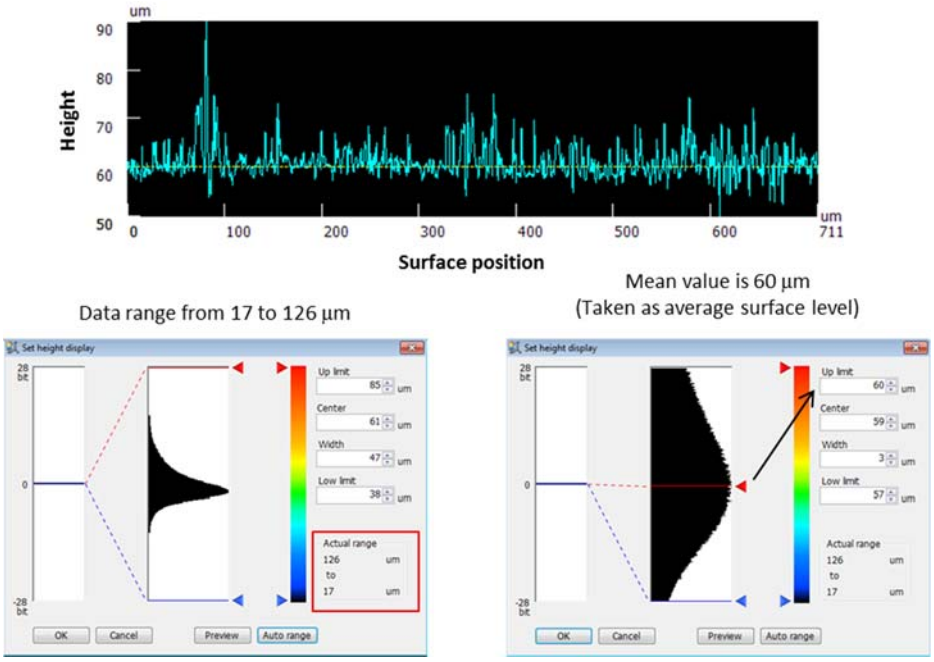

Figure 17. LCM software screen shots showing an example representing a surface with height data range between 17 and 126 µm and a mode value of 60 µm.

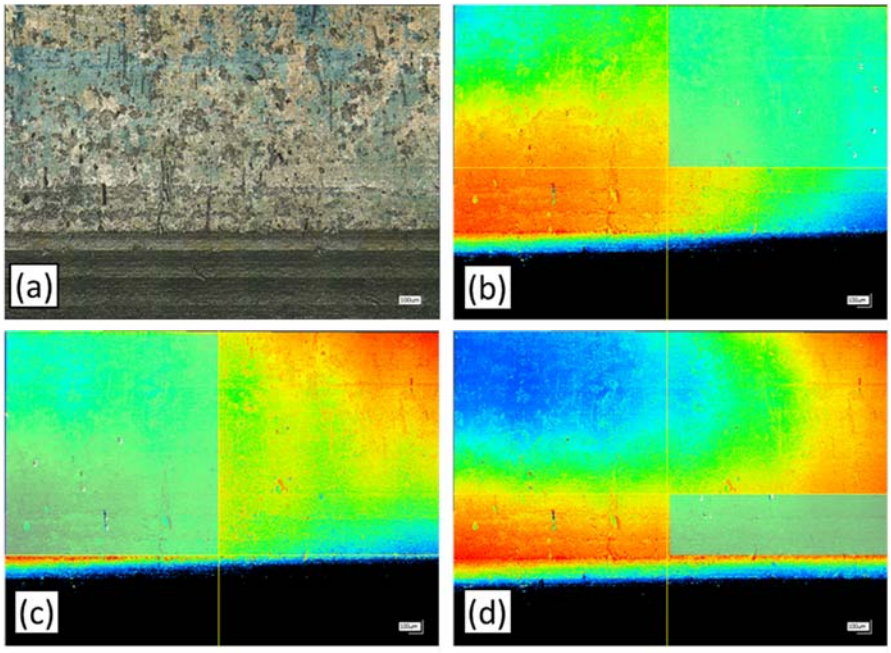

Figure 18. LCM analysis using the BMM for Region 3 of FY09 DE02-270° ICCWR sidewall sample showing (a) the optical images montage, and green-shaded sections on height scans indicating tilt correction base on (b) top-right quadrant, (c) left-half section, and (d) lower-right quadrant. Increasing height is represented by transition in color from blue (lowest) to red (highest).

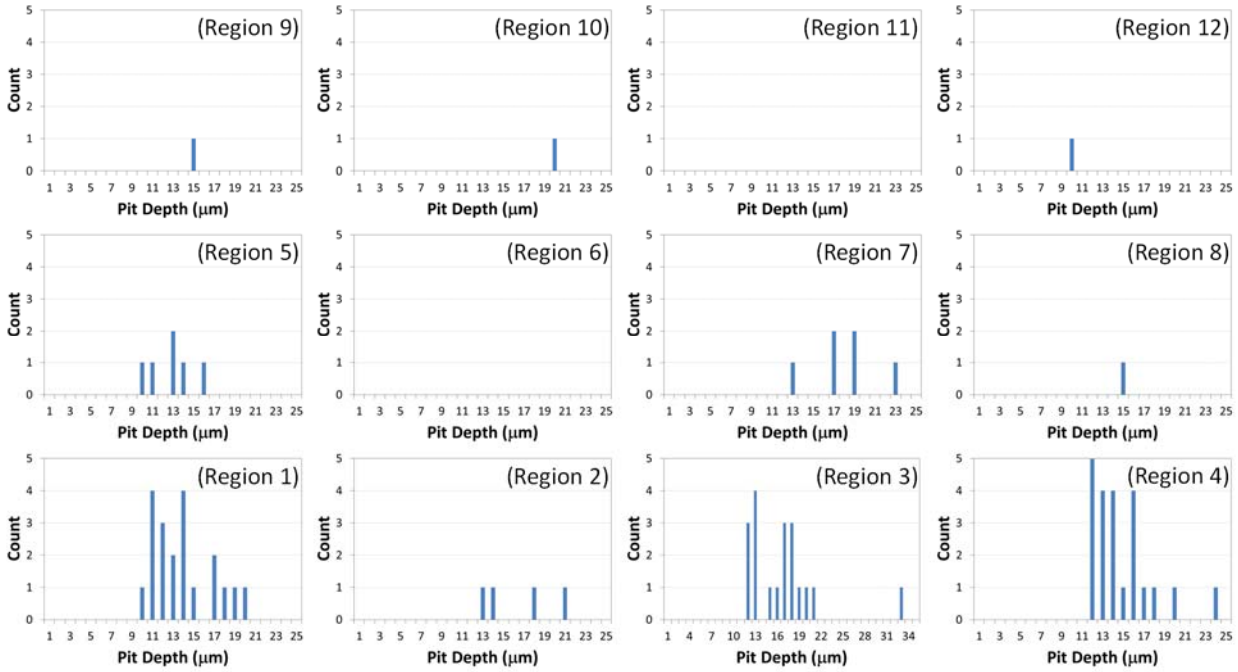

Figure 19. Pit depth distributions for FY09 DE02-270° ICCWR sidewall sample obtained with the BMM for each of the 12 regions displayed in Figure 16.

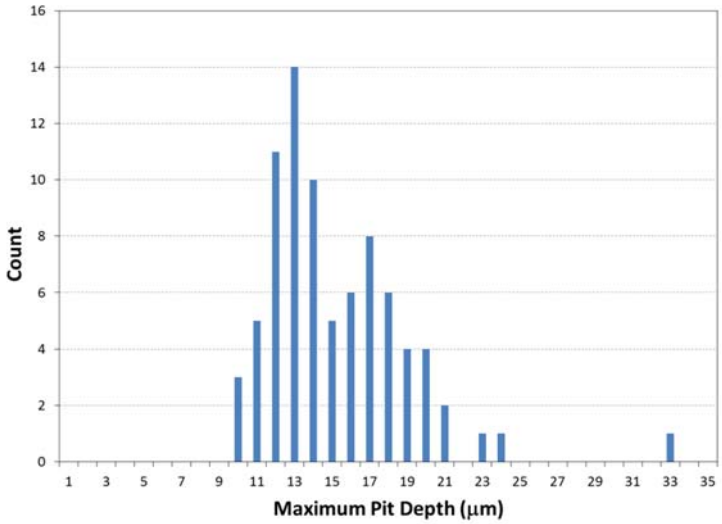

Figure 20. Overall pit depth distributions for FY09 DE02-270° ICCWR sidewall sample. This plot represent the total count summary for the results shown in Figure 19.

3.2 ICCWR Examination of FY11 HHMC

FY11 HHMC is the inner container known for the high moisture condition during storage and the amount of corrosion and pitting found [2]. This container was selected for analysis of a significant larger region of the ICCWR. Figure 21 shows the interior of the inner container top lid with a quarter labeled as Section B. This section was further cut into Sections B-1, B-2 and B-3 for analysis of the ICCWR by LCM. Similar to FY09 DE02-270° sidewall, the analysis was performed up to about 6 mm in Zone 3 from the machining marks towards the bottom of the can. A view of

Section B-3 is shown in Figure 22. The section is about 23.3 mm wide. It shows a rough surface in Zone 3 and partial loss of the HAZ tint due to corrosion along the bottom of Zone 3 (bottom of the image).

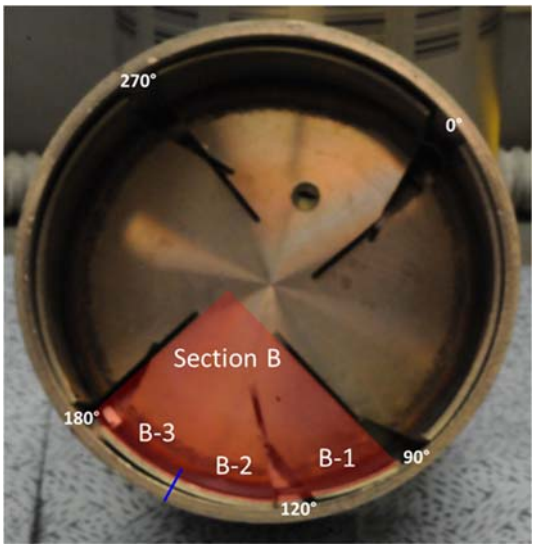

Figure 21. Inner container top lid of FY11 HHMC showing the section cut for examination of the ICCWR. Sections B-1 to B-3 correspond to samples used for LCM analysis. The sections with degrees correspond to samples used for metallography analysis.

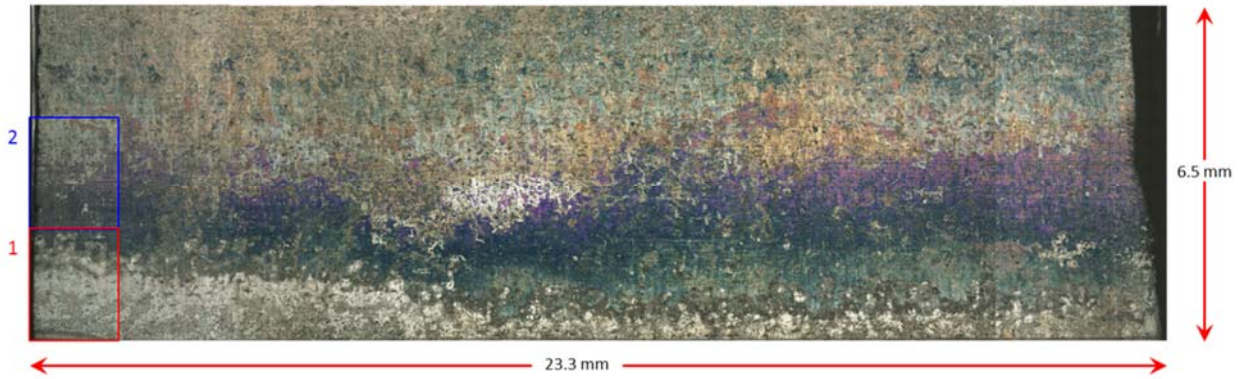

Figure 22. Optical image of FY11 HHMC-B3 ICCWR sidewall showing Zone 3 (region measuring 6.5 mm above machining marks). Note that the picture is oriented such that the weld (not shown) is below Zone 2. Box labeled as region 1 and 2 correspond to image sections shown in Figure 23 and Figure 24 respectively.

The regions 1 and 2 shown in Figure 22 were analyzed using the BMM. The corresponding analyses are shown in Figure 23 and Figure 24, respectively. Each figure shows the optical image for the corresponding region where some baseline features can be observed. Also, the height scan is presented indicating with arrows some deeper features found on the surface. These deeper features cause the BMM to identify many concave features as shown by the white marks in Figure 23(c) and Figure 24(c). The depth distributions of these concave features are shown in Figure 25 for regions 1 and 2. The depth ranges between 11 μm and 27 μm with a mode of 17 μm for region 1 and a mode of 13 μm for region 2. This conglomerate of features shows up as a large cluster of

pits. On the other hand, some other portions of the sample do not show concave features as the surface is mostly flat. However, the evenness of the surface corresponds to the section where the HAZ tint was lost due to the amount of corrosion that resulted in the removal of the top surface. Further analysis of these samples is still needed to evaluate pits. Also, an alternative technique is being investigated to process the data collected from the LCM. However, these results show that the corrosion can be extended as far as 6 mm in Zone 3.

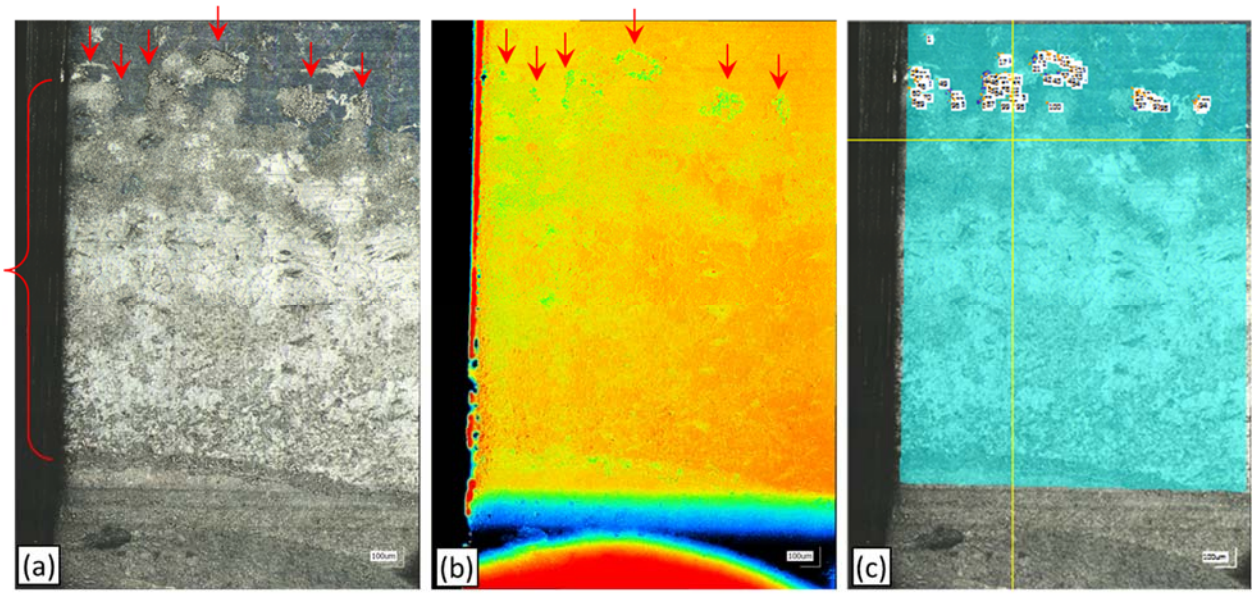

Figure 23. LCM analysis using the BMM for Region 1 of FY11 HHMC-B3 ICCWR sidewall sample showing (a) the optical images montage, (b) the height scan, and (c) and the BMM results. Increasing height is represented by transition in color from blue (lowest) to red (highest). The white marks in (c) correspond to concave features identified by the software.

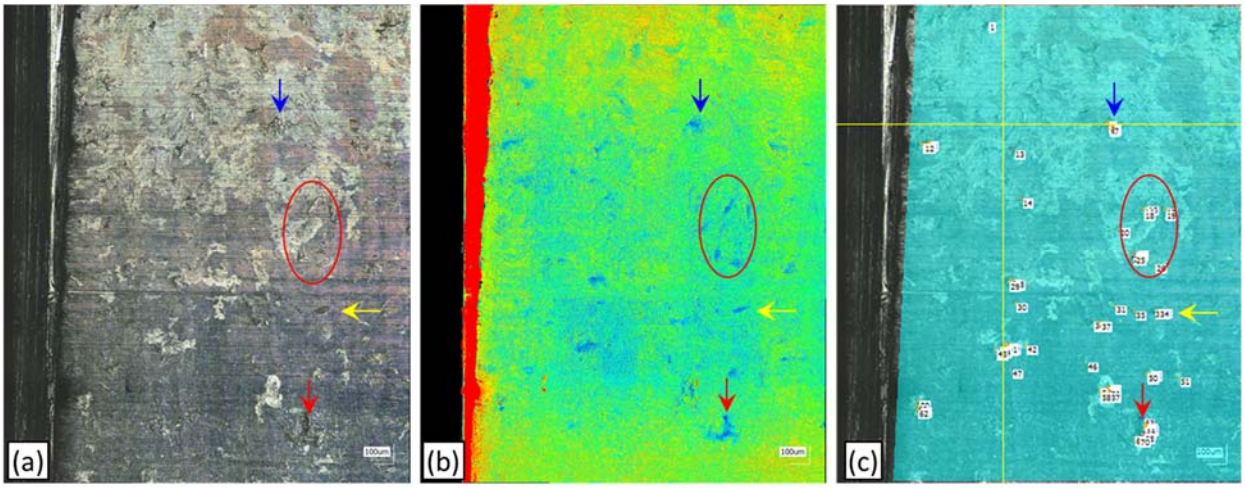

Figure 24. LCM analysis using the BMM for Region 2 of FY11 HHMC-B3 ICCWR sidewall sample showing (a) the optical images montage, (b) the height scan, and (c) and the BMM results. Increasing height is represented by transition in color from blue (lowest) to red (highest). The white marks in (c) correspond to concave features identified by the software.

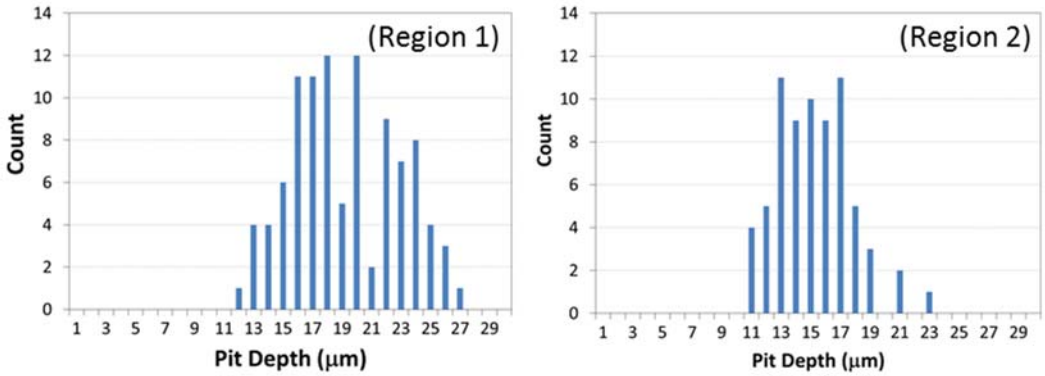

Figure 25. Pit depth distributions for FY11 HHMC-B3 ICCWR sidewall sample obtained with the BMM for regions 1 and 2 displayed in Figure 22.

4.0 DE Containers Evaluation for ICCWR Full Circumference Examination

When the LCM was introduced, as part of the ICCWR protocol [3], only small areas where examined and an improved LCM technique was required to address the challenges described in this report regarding the collection and analysis of the data. During the development of the LCM technique for analysis of the ICCWR in DE samples, a backlog of DE containers has been created since FY13. In order to analyze the ICCWR for the backlog and future DE containers, defined as production mode, a statistical model is being developed with LANL to determine the minimum data collection requirements to make the assertion of whether or not cracking has occurred. During the production mode, only the minimum sampling size of the ICCWR area will be analyzed by LCM.

As part of the statistical model development, the ICCWR from several DE containers are required to be analyzed by LCM around the full circumference. This analysis will be used to provide information about the distribution of the corrosion features of interest [16]. If the corrosion features are randomly distributed then a random section from each DE container is sufficient for production mode. However, the size of the section needs to be determined such as to have a high confidence of capturing the corrosion features. If the corrosion features are not randomly distributed (i.e. clustered) then auxiliary information, such as stereo microscope images, is needed to determine the areas to be scanned and analyzed. In this case, the auxiliary information needs to be correlated with the LCM data.

DE containers from FY13 through FY16 were evaluated to select three candidates for the full circumference analysis of the ICCWR. Although the MIS Corrosion Working Group recognized the need to examine a baseline un-corroded container for comparison to cases where corrosion occurred in storage it was agreed that a baseline container would not be included as one of the three candidates. The reason is because the objective of this analysis is to determine the distribution of the corrosion features. The DE containers were evaluated using 35 mm pictures, stereo microscope images, and the standard corrosion categorization to judge the most likely inner containers to show corrosion features of interest in the ICCWR. Table 2 shows a summary of the DE containers divided in three groups: (1) not selected, (2) honorable mention, and (3) finalists. The standard categorization for each DE container set is indicated in Table 2 with the definitions of each category given in Table 3.

Table 2. Summary of containers selection for ICCWR full circumference examination.

DE ID		Standard Categorization	Not Selected	Honorable Mention	Finalist
FY13	DE01	6		x	
FY14	DE01	0	x		
	DE02	3A	x		
	DE03	3A	x		
	DE04	3A	x		
	DE05	3A	x		
	DE06	0	x		
	DE07	0	x		
	DE08	4		x	
	DE09	0	x		
FY15	DE01	0*	x		
	DE02	0	x		
	DE03	0	x		
	DE04	0		x	
	DE05	6		x	
	DE06	5		x	
	DE07	5			x
	DE08	5			x
	DE09	3A	x		
FY16	DE01	0	x		
	DE02	6		x	
	DE03	6+			x
	DE04	3A	x		
	DE05	6			x
	DE06	3A	x		

Table 3. Standard corrosion categorization for 3013 containers.

Category	Description
0	Nothing or wipeable coating
0*	RF and LL can if corrosion is observed
1	Adherent coating on convenience can
2	Pitting <50 µm on convenience can
3A	Suspect pitting > 50 µm on convenience can – pit covered with corrosion products
3B	Confirmed pitting > 50 µm on convenience – generally confirmed with SEM
4	Adherent coating on inner can
5	Pitting < 50 µm on inner can
6	Pitting > 50 µm on inner can
7	SCC in the inner can

The three candidates for the full circumference analysis of the ICCWR were selected as those likely having more corrosion features in this region. DE inner containers that did not show signs of corrosion were not selected. Generally, this group corresponds to DE containers with categories 3B and below. These categories are assigned to DE containers with corrosion features in the convenience container which also correspond to DE containers that do not show corrosion in the inner container. Honorable mention is the group of DE containers with categories 4 and above which have corrosion features but these features occur in less magnitude than the DEs selected as finalist. Categories 4 and above correspond to the containers with corrosion features such as adherent coating and pitting in the inner can. The containers selected as honorable mention are FY13 DE01, FY14 DE08, FY15 DE05, FY15 DE06 and FY16 DE02. However, with the images available, FY15 DE04 (category 0) did not show evidence of corrosion in the inner container but it showed signs of possible or suspect corrosion, which need to be evaluated in more details after accessing the ICCWR. Figure 26 shows the interior surface of the inner container top lid. The gap of the ICCWR has a wide separation and several yellow stains are close to this gap region. Consequently, this DE was selected as honorable mention as well. Some DE containers in the honorable mention group have a higher category than the finalist group because they showed a few pits larger than 50 μm in the inner container but still the magnitude of corrosion features is less than the finalist group.

The finalist group contains the candidates for the full circumference analysis of the ICCWR. The DE containers in the finalist group are FY15 DE07, FY15 DE08, FY16 DE03 and FY16 DE05. Images of these DE containers are shown in Figure 27 through Figure 30, respectively. For these DE containers, all the convenience containers have an adherent coating, except for FY15 DE08 which had a removable coating. A coating was also observed on the sidewalls of the inner container for FY15 DE07 (Figure 27a). However, this coating was removable. In the inner container, locations with suspect corrosion features are indicated with red and white arrows. These corrosion features are not completely clear from the figures but they are more noticeable when the images are zoomed-in. These corrosion features correspond to stains and a coating or general corrosion close to the gap region. Also, the stereomicroscope images for all the inner container top lids show pitting or suspect pitting (white arrows) on the interior surface. These DE containers are standard category 5 or higher with signs of suspect corrosion near the gap region.

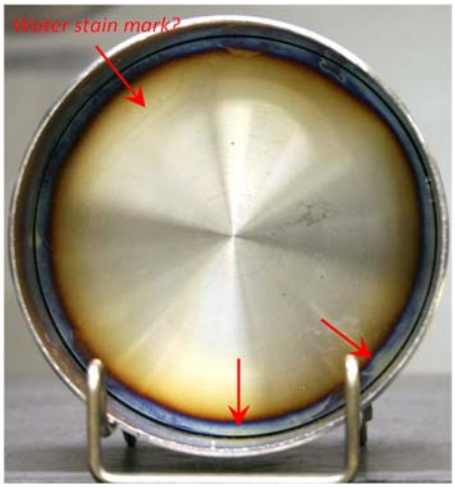

Figure 26. FY15 DE04 image for inner container top lid. The ICCWR has a wide separation and several yellow stains are close to this gap region as indicated with the red arrows.

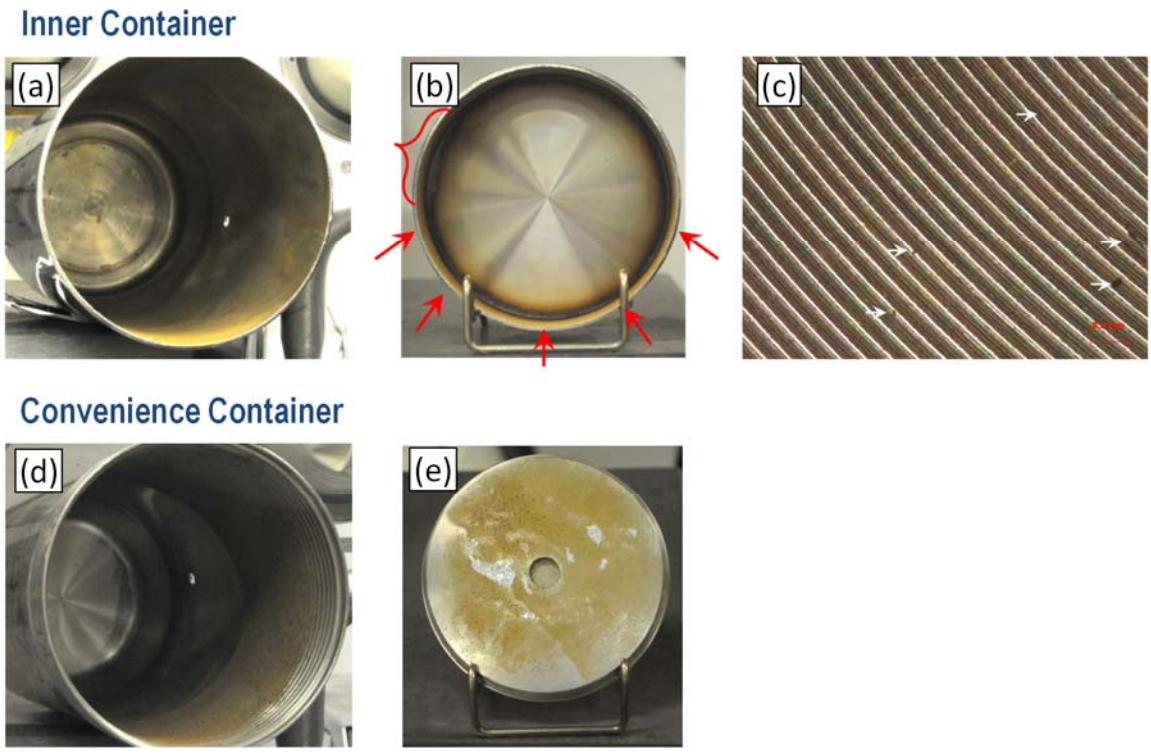

Figure 27. FY15 DE07 images for (a) inner container body and (b) lid; (c) stereo microscope image at 25X of inner surface of lid, and images of (d) convenience container body and (e) lid.

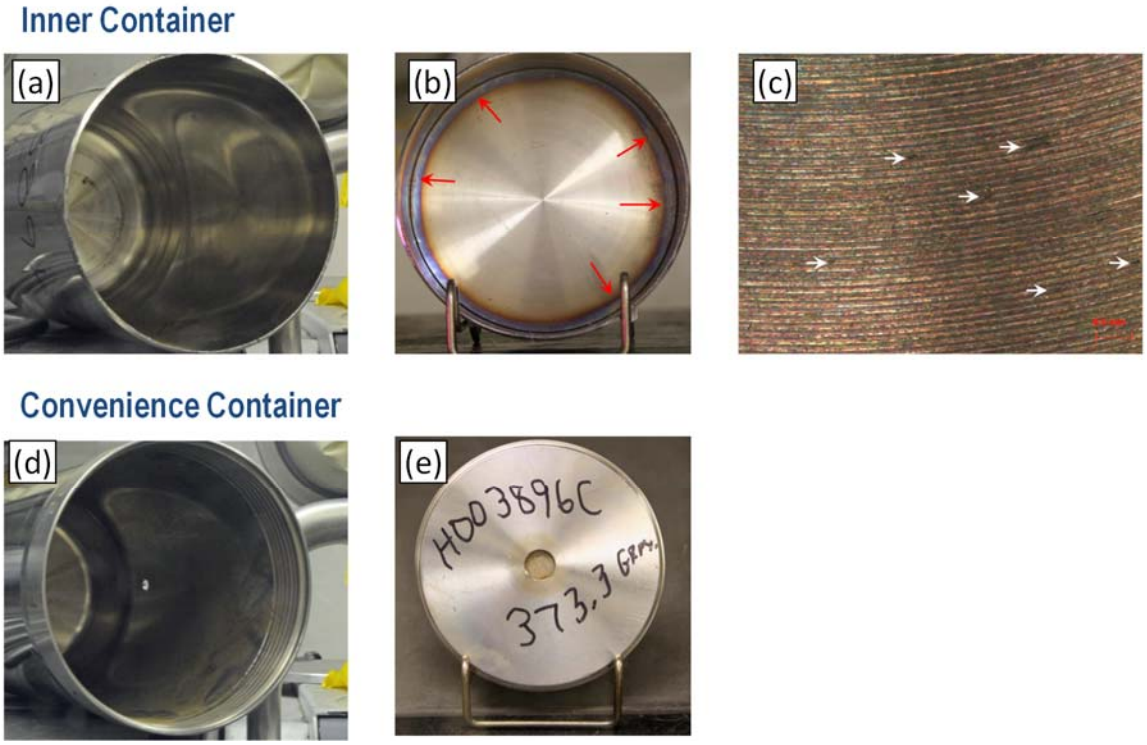

Figure 28. FY15 DE08 images for (a) inner container body and (b) lid; (c) stereo microscope image at 25X of inner surface of lid, and images of (d) convenience container body and (e) lid.

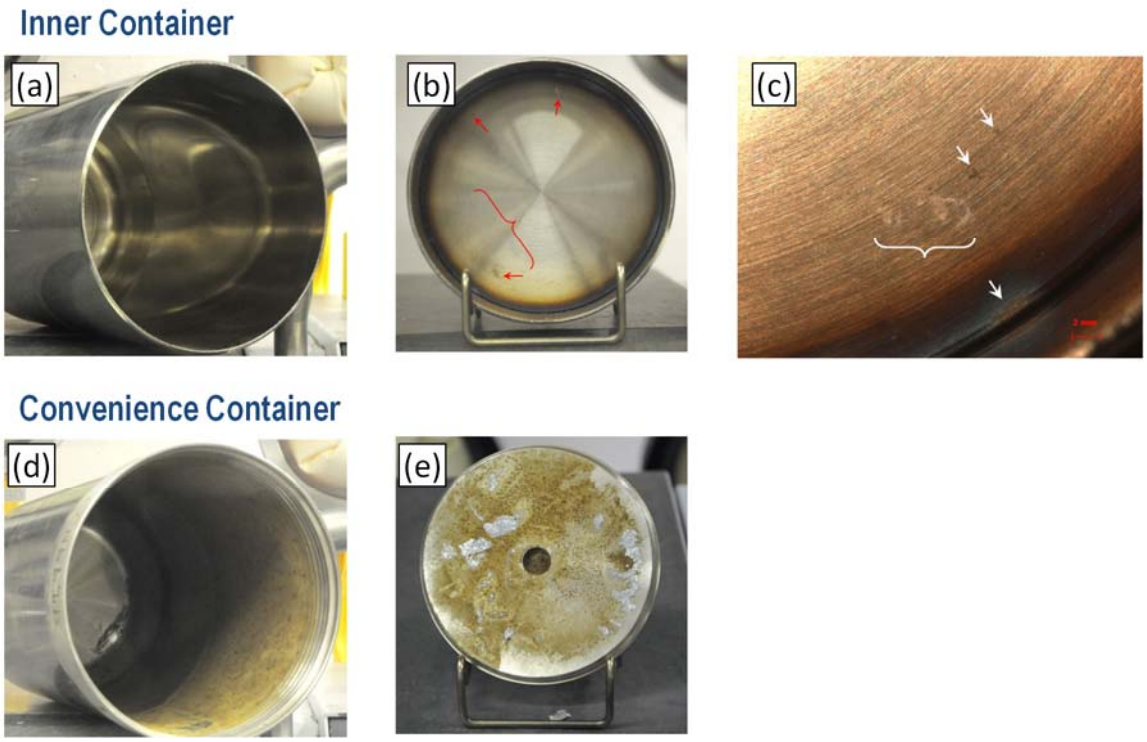

Figure 29. FY16 DE03 images for (a) inner container body and (b) lid; (c) stereo microscope image at 5X near gap region, and images of (d) convenience container body and (e) lid.

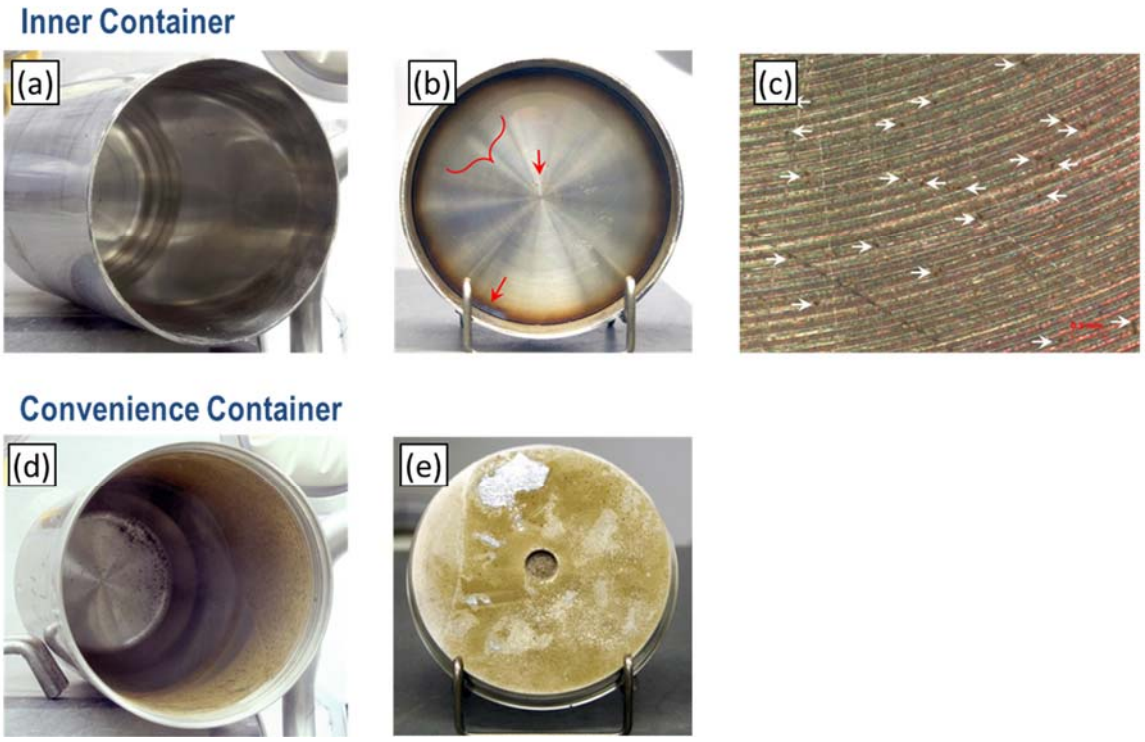

Figure 30. FY16 DE05 images for (a) inner container body and (b) lid; (c) stereo microscope image at 25X of inner surface of lid, and images of (d) convenience container body and (e) lid.

From the four containers binned as finalists, the MIS Corrosion Working Group indicated that FY16 DE3 will not be selected for the initial round of full circumference examinations. This container has some indications of corrosion on the outside of the inner container lid. It was agreed that this lid should be saved intact for a possible helium leak check if this capability is fully developed and implemented at SRNL. The three remaining finalist DE containers were selected for full circumference analysis of the ICCWR with the following prioritization order: FY15 DE07, FY16 DE05, and FY15 DE08. FY15 DE07 was selected as the first priority because it is the only DE, from the DEs evaluated up to FY16, that showed a coating on the sidewalls of the inner container. FY16 DE05 was selected as the second priority because it showed a large number of pits on the interior surface of the inner can top lid compared to FY15 DE08. In addition, it is possible to replace FY15 DE08 from among the honorable mention or other containers from FY17 if not much corrosion is found in the ICCWR. However, this can be re-evaluated at some point in the future before FY15 DE08 is examined.

5.0 Conclusions

As part of the protocol to investigate the corrosion in the ICCWR, an LCM was used to perform close visual examination of the surface and measurements of corrosion features on the surface. Challenges of this examination include topography of the ICCWR sample, surface features, and the amount of surface area for collecting data at high magnification conditions. Consequently, an analysis was performed on selected DE inner containers to identify the appropriate parameter values for data acquisition and identification of regions of interest and to determine the extent of the ICCWR examination.

- Based on the information presented in this report the following basic parameters were selected for the examination of the ICCWR with detection of cracks of, at least, 1 μm.

    1. Zone 3 image and height data will be collected using 20X magnification, with the double scan function disabled, measurement area set to standard, quality set to high accuracy and, a pitch value of 0.5 μm.

    2. Zone 1 and Zone 2 will be examined but images or height data will not be collected unless areas of interest are found. These areas of interest correspond to sections where suspect cracks, significant number of pits or other corrosion features are located. If data collection is necessary for Zone 1 and Zone 2, the double scan function will be enabled.

    3. If higher resolution is desired, the parameters can be adjusted accordingly for specific areas of interest.

- The BMM can be used to expedite analysis for evaluation of general condition of the surface but does not distinguish between cracks, scratches or pits. Due to the shallow depth of the baseline container features the BMM can be used to analyze the deeper corrosion features or pits. However, additional tilt correction may be needed in smaller locations, even after assembling sections of several images, due to curvature of the sample and the uneven surface.

- Results from this report show that the corrosion can be extended as far as 6 mm in Zone 3. However, no cracks were detected within the data analyzed.

- Based on the results obtained to date the following DE containers were selected for full circumference analysis of the ICCWR with the following prioritization order: FY15 DE07, FY16 DE05, and FY15 DE08. However, this selection can be re-examined and may change in the future as new information becomes available.

6.0 References

1. Berg, J.M., D.K. Veirs, E.J. Kelly, Juan G. Duque, S.A. Joyce, J.E. Narlesky, J.M. Duffey, J.I. Mickalonis, and K.A. Dunn, *Test Plan for Assessing Potential for Stress Corrosion Cracking in the 3013 Inner Container Closure Weld Region (FY 2014).* 2014, LA-UR-14-20785.
2. Mickalonis, J.I., *3013 DE Inner Container Closure Weld Corrosion Evaluation.* 2013, SRNL-STI-2013-00527.
3. Mickalonis, J.I. and K.A. Dunn, *Protocol for Examination of the Inner Can Closure Weld Region for 3013 DE Containers.* 2014, SRNL-L4400-2014-00020.
4. Mickalonis, J.I. and G.T. Chandler, *Status of the Examination of the Inner Container Closure Weld Region for FY13 and FY14 3013 DE Containers.* 2015, SRNL-L4400-2015-00020.
5. Martínez-Rodríguez, M.J., *Status of the Examination of the Inner Container Closure Weld Region for Selected 3013 DE Containers.* 2016, SRNL-L4400-2016-00021.
6. Duncan, A.J., P.-S. Lam, R.L. Sindelar, and J.T. Carter. *Crack Growth Rate Testing With Instrumented Bolt-Load Compact Tension Specimens Under Chloride-Induced Stress Corrosion Cracking Conditions in Spent Nuclear Fuel Canisters*. in *Proceedings of the ASME 2017 Pressure Vessels & Piping Conference Pressure*. 2017. Waikoloa, Hawaii , United States: ASME.
7. Mickalonis, J.I., *Assessment of Residual Stresses in SRS and Hanford 3013 Inner and Convenience Cans.* 2009, SRNL-STI-2009-00121.
8. Rios, D., J.M. Berg, J. Duque, D. Tung, D.K. Veirs, and L.A. Worl, *Corrosion on 304L SS Teardrops Exposed to Chlorine-Containing Gases in Aerobic and Anaerobic Environments.* Unpublished report to be submitted.
9. Keyence, *3D Laser Scanning Microscope VK-X100K/X200K Training Manual*. 2012.
10. Mickalonis, J.I. and K.A. Dunn, *Residual Stresses in 3013 Containers.* Journal of Nuclear Materials Management, 2010, **38**: p. pp 31-38.
11. Stroud, M.A., M.B. Prime, D.K. Veirs, J.M. Berg, B. Clausen, L.A. Worl, and A. DeWald, *Assessment of Residual Stresses in 3013 Inner and Outer Containers and Teardrop Samples.* 2015, LA-UR-15-29376.
12. Duque, J., K. Kaufeld, and E. Kelly, *Baseline Data Depth Analysis and Implications for DE Data Collection and Analysis*. 2017, Presentation for the Corrosion Working Group Call on June 22, 2017.
13. Kelly, E.J., T.L. Graves, D.K. Veirs, J.G. Duque, J.M. Berg, L.A. Worl, and J.I. Mickalonis, *A General Statistical Model for Corrosion Pit Depth Analysis for Threshold Data.* 2013, LA-UR-13-25127.
14. Keyence, *3D Laser Scanning Microscope VK-X100K/X200K VK Viewer/VK Image Stirching Reference Manual*. 2012.
15. Keyence, *3D Laser Scanning Microscope VK-X100K/X200K VK Analyzer Reference Manual*. 2012.
16. Kelly, E., *Using Initial LCM 20X Scans of ICCWR to Focus "Production-Mode" Scans.* 2017, Presentation at Corrosion Working Group Meeting on February 2, 2017.

Appendix A. LCM Data Resolution

This Appendix shows the LCM image resolution as function of assembled images in the x and y directions. The assembly process was tested with the image data of FY09 DE02-270° ICCWR sidewall sample from Figure 16 in which image sections, indicated by the boxes shown in Figure 31, were reassembled. The individual images have a standard resolution of 1024 pixels in the x-direction and 768 pixels in the y-direction. During the image assembly, the maximum image size resolution available in the software was always selected for investigating the number of pixels in the final assembly. Several images were reassembled in the x-direction, y-direction and x-y simultaneously while accounting for the number of pixels in the final assembled images. The number of pixels in the final assembled images was compared to the expected pixels in order to detect any decrease in resolution of the image. As part of the data collection process, the software overlaps partially the individual images. Therefore, there is an expected decrease in the number of pixels in the final assembled image, which is not related to loss of image resolution.

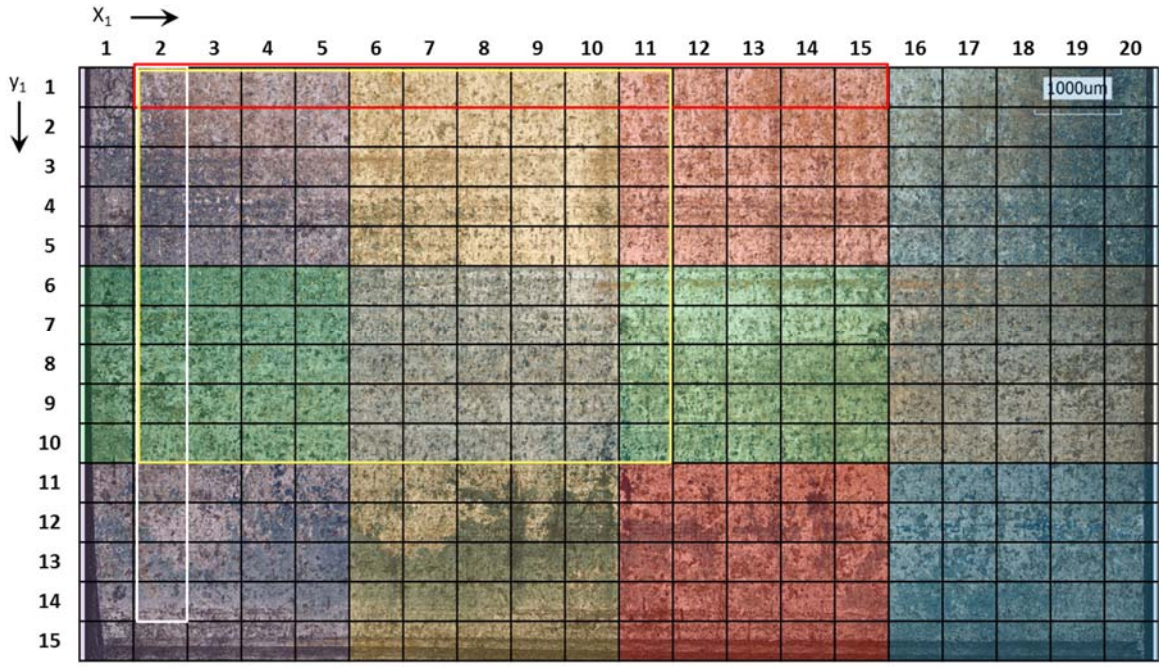

Figure 31. LCM image assembly composed of 300 individual images for FY09 DE02-270° ICCWR sidewall sample showing direction of reassembled images in the x-direction (red box), y-direction (white box) and x-y matrix (yellow box).

Figure 32 and Figure 33 shows the calculation of the overlapped pixels for the image assembly in the x-direction and y-directions, respectively. Figure 34 to Figure 36 show the pixels count as function of the number of assembled images in the x, y, and simultaneous x-y directions. Up to 14 images were assembled in the x or y directions showing only a constant percent overlap which corresponds to 128 pixels/image. The overlap in the x-direction is 12.5% and the overlap in the y-direction is 16.7%. However, when the images are assembled in x-y directions simultaneously, the percent overlap shows an increase to about 61% - 66% after an assembly of 6 x 6 individual images. The increase in overlap percent is not due to an additional overlap of pixels in the images but it occurs because a specific number of pixels are missing in the final assembled image. This loss of pixels causes a reduction in the image resolution. This is consistent with the LCM reference

manual which describes the reduction in image resolution when the vertical x horizontal exceeds 25,160,256 pixels [14]. The final resolution (after accounting for overlap) of the 6 x 6 assembly is 21,996,279 pixels. The 7 x 7 assembly exceeded the software pixel limit and resulted in a final resolution of 7,420,104 pixels. Consequently, the maximum number of images that can be assembled is a matrix of 6 x 6.

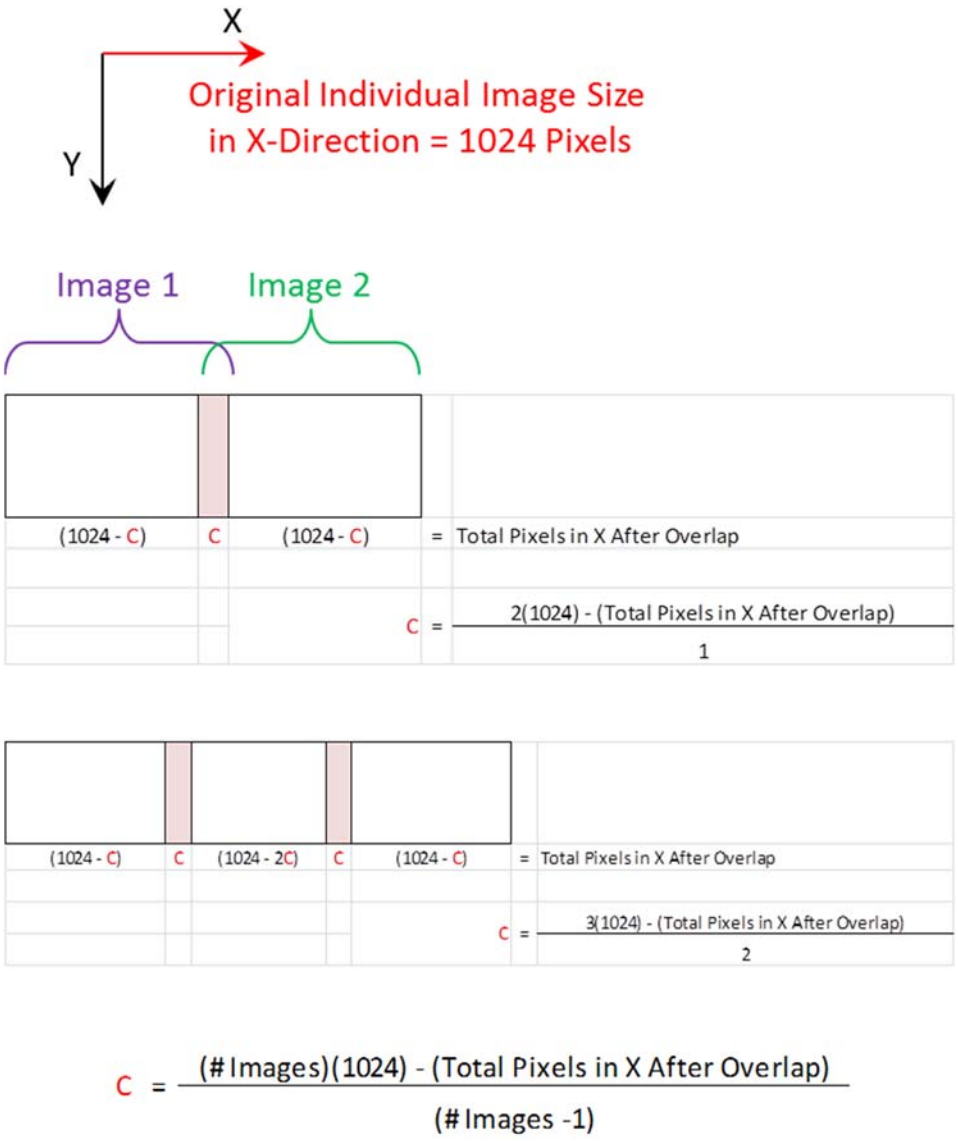

Figure 32. Sketch showing the image overlap and the overlapped pixels calculation (C) for the image assembly in the x-direction.

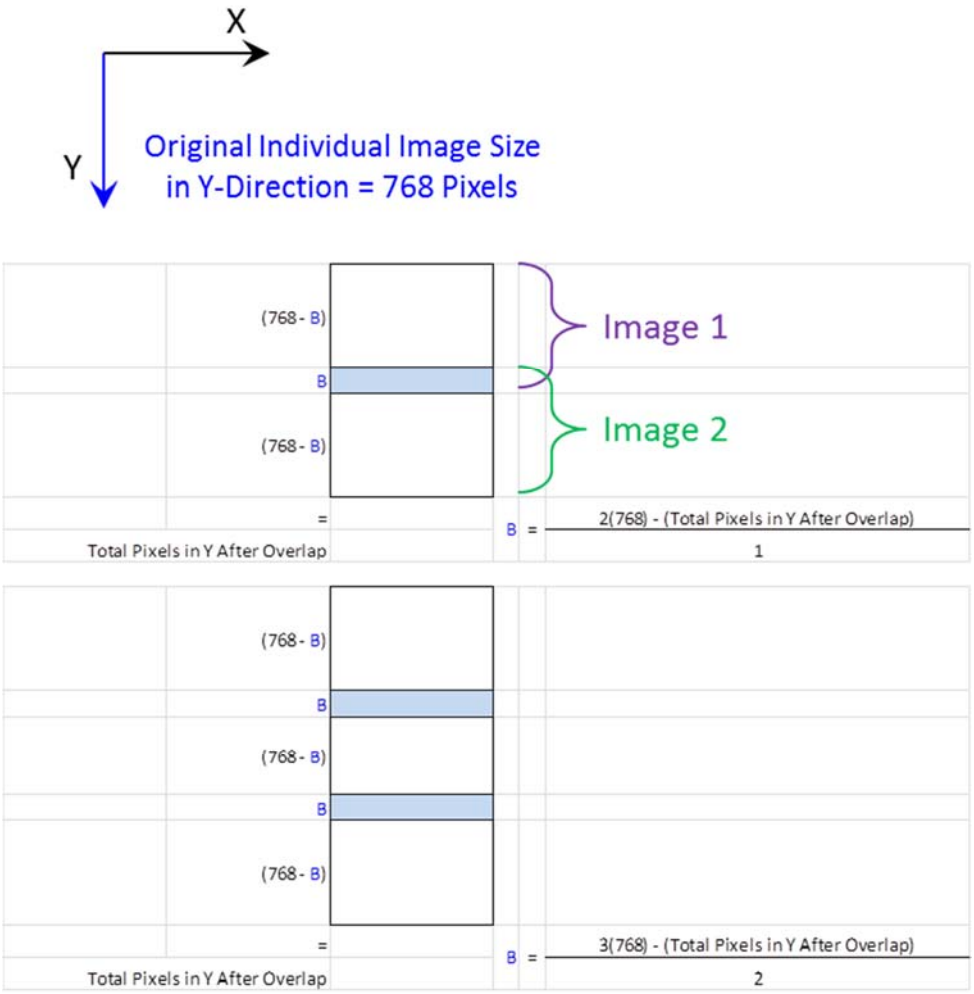

$$B = \frac{(\#\ \text{Images})(768) - (\text{Total Pixels in Y After Overlap})}{(\#\ \text{Images} - 1)}$$

Figure 33. Sketch showing the image overlap and the overlapped pixels calculation (B) for the image assembly in the y-direction.

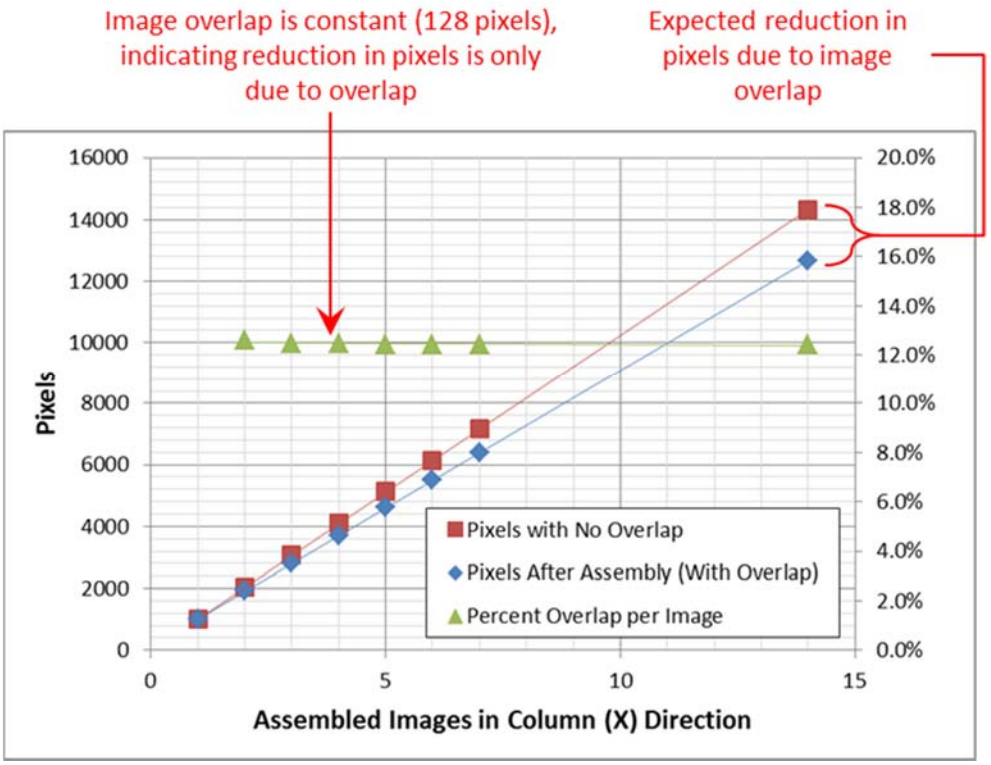

Figure 34. Pixels count as function of the assembled images in x-direction.

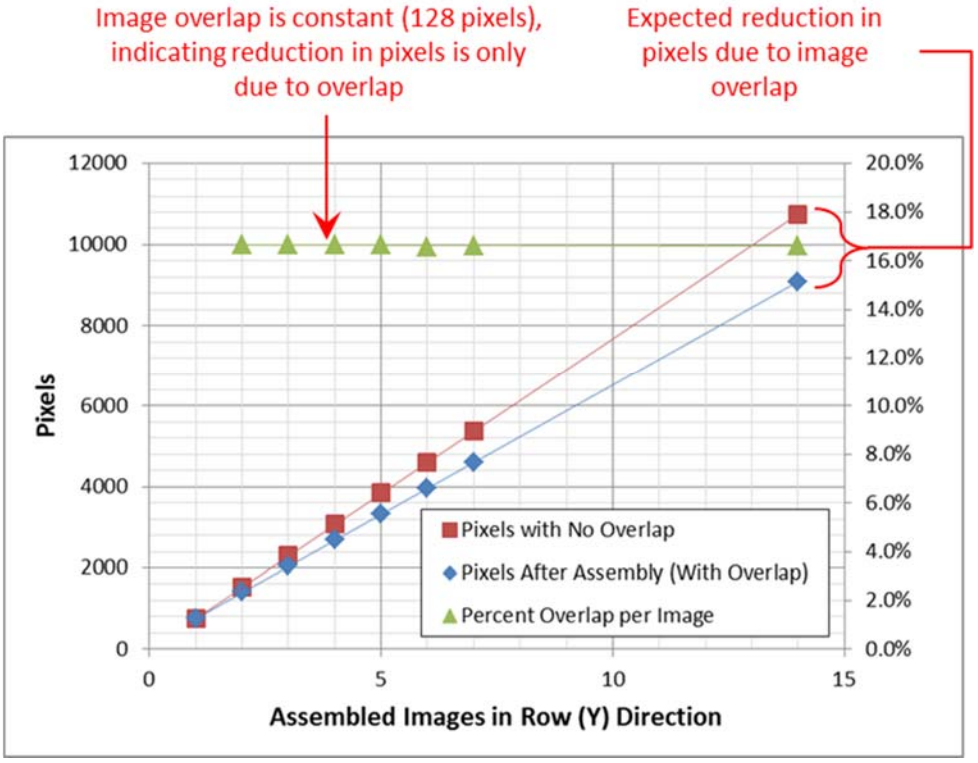

Figure 35. Pixels count as function of the assembled images in y-direction.

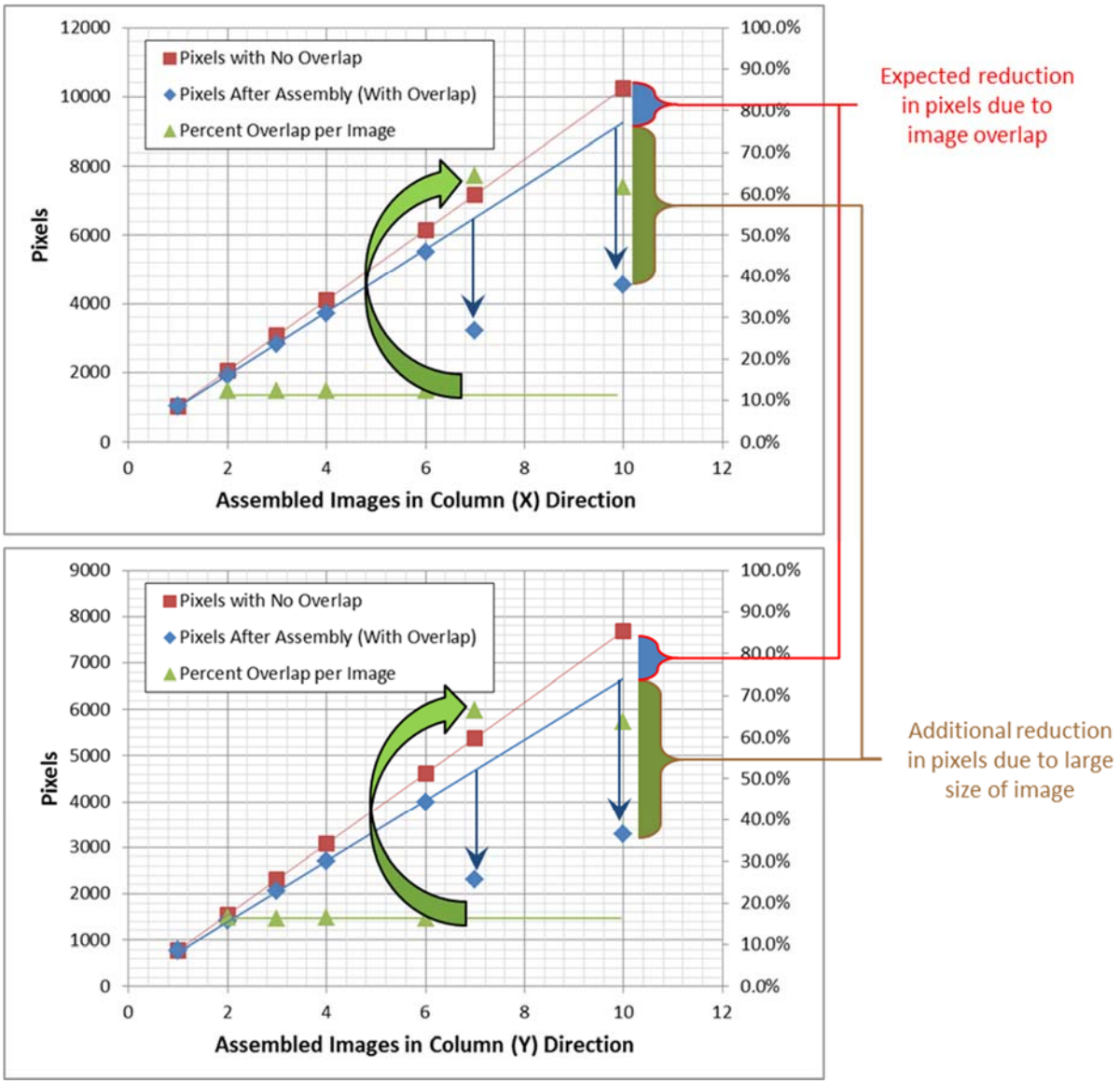

Figure 36. Pixels count as function of the assembled images in x and y-directions simultaneously.